General Disclaimer

One or more of the Following Statements may affect this Document

- This document has been reproduced from the best copy furnished by the organizational source. It is being released in the interest of making available as much information as possible.

- This document may contain data, which exceeds the sheet parameters. It was furnished in this condition by the organizational source and is the best copy available.

- This document may contain tone-on-tone or color graphs, charts and/or pictures, which have been reproduced in black and white.

- This document is paginated as submitted by the original source.

- Portions of this document are not fully legible due to the historical nature of some of the material. However, it is the best reproduction available from the original submission.

Produced by the NASA Center for Aerospace Information (CASI)

DOE/NASA/3249-1
NASA CR-168080

Vaporization Thermodynamics of K$_2$S and K$_2$SO$_3$

J. Edward Bennett
Arkansas State University

June 1982

Vaporization Thermodynamics of K_2S and K_2SO_3

J. Edward Bennett
Arkansas State University
State University, Arkansas 72467

June 1982

PREFACE AND ACKNOWLEDGEMENTS

Arkansas Academy of Sciences, Little Rock, April, 1981; one paper at the 66th Annual Meeting of the Arkansas Academy of Sciences, Arkadelphia, April, 1982; one paper at the Ninth Midwest High Temperature Chemistry Conference, Los Alamos National Laboratory, June, 1981; and a paper on the collaborative results from Lewis Research Center, the University of Toledo, and Arkansas State University at the National Meeting of the Electrochemistry Society, Denver, Colorado, October, 1981. (This paper was presented by Dr. Fred Kohl.)

TABLE OF CONTENTS

PRINCIPAL INVESTIGATOR'S SUMMARY

The objective of this project was to investigate the high temperature thermodynamics of potassium sulfite (K_2SO_3) and of potassium sulfide (K_2S) for purposes of application to the seed chemistry of open-cycle, coal-fired magnetohydrodynamic (MHD) electric power generation. The program involved three stages: (1) construction of an experimental facility to permit vapor pressure measurements in vacuum at high temperatures; (2) high temperature studies of K_2SO_3; (3) high temperature studies of K_2S.

The Knudsen rate-of-effusion method was used to obtain data for subsequent vapor pressure and related thermodynamic calculations. In this method the sample was caused to vaporize in vacuum by effusion through a small orifice in an otherwise closed containing vessel (the Knudsen cell). Several materials were evaluated for use as Knudsen cells above $800^{\circ}C$: platinum, boron nitride, machinable glass, tungsten, molybdenum, alumina, high density graphite, and pyrolytic-coated graphite. Of these materials, only graphite proved suitable for K_2S, and none proved completely satisfactory for K_2SO_3 (alumina is apparently chemically inert to both K_2SO_3 and K_2S, but small samples, 10 to 100 mg, showed anomalous effusion behavior in alumina, suggesting surface interactions).

The rate-of-effusion studies, supported by tube furnace experiments, X-ray powder diffraction, mass spectrometry, and chemical analyses and tests as appropriate, revealed the following new knowledge about K_2SO_3 and K_2S:

(1) K_2SO_3 undergoes a disproportionation reaction at high temperatures to form K_2S and K_2SO_4. Subsequent vaporization first involves the K_2S formed. Thus K_2SO_3 vaporizes incongruently.

(2) When K_2S is vaporized in vacuum, the initial vapors are predominantly potassium atoms, with minor species being S_2 and various K-S molecules. The ratio of K/S_2 in the vapor is very large initially and decreases steadily with prolonged heating. Thus K_2S also vaporizes incongruently.

Chemical reactions were established from the above facts, and measured vapor pressures, interpreted accordingly, provide new values for the standard heat of formation of K_2S. Appropriate equilibrium constant expressions and free energy functions were also obtained. Auxillary results include measurements of the vapor pressure of silver (used for system verification), and of $K_2S_2O_5$ (used as a thermal decomposition source for K_2SO_3).

The results for K_2SO_3 in graphite containers should be of great interest to MHD, in this investigator's opinion. Evidence was obtained for a reduction reaction that has potential application as a short-cut in the seed reprocessing procedure. The reaction would be useful regardless of the K-S-O composition emerging from the MHD generator. Further work is suggested along this line, particularly studies of the K_2SO_4-graphite system.

1. INTRODUCTION

1.1 BACKGROUND

In proposed coal-fired, open-cycle magnetohydrodynamic (MHD) electrical power generating systems, plans call for doping the combustion stream with a "seed" compound, potassium carbonate (K_2CO_3), for the purpose of producing gaseous potassium ions (K^+) as electric current carriers in the MHD generator. A preliminary evaluation of the problems involved in predicting and controlling the fate of gaseous K^+ ions in cooling MHD streams was reported previously (Ref. 1). The two main ideas of that study which led to further experimental work reported here were:

(1) A high percentage (ideally 100%) of the potassium must be recoverable for subsequent re-use, thus effecting a virtual closed-cycle for the seed compound, K_2CO_3.

(2) Potassium ions emerging from the MHD generator would be exploited as "getters" for fuel-derived sulfur-bearing species in the cooling stream. They would cause the precipitation of potassium sulfate (K_2SO_4) under conditions of oxidant-rich combustion, and of reduced forms such as potassium sulfite (K_2SO_3) and/or potassium sulfide (K_2S) from fuel-rich combustion.

It should be noted that the requirement for using the seed compound to remove sulfur on a continuous basis necessitates a seed-regenerating process in which the sulfur is separated from the seed products in usable form, while in the same process potassium is returned to K_2CO_3. Otherwise, the seed compound could be simply K_2SO_4 from start to finish, and

1

the sulfur from the fuel could be removed downstream by conventional means. Recommending between these alternative approaches for the seed cycle has been impossible because of the lack of reliable data on the high temperature chemistry of the potassium-oxygen-sulfur system. No MHD generator has been operated in a manner that uses a seed compound to remove sulfur. And though some predictions were made during the British MHD program (Ref. 2) regarding conditions for the precipitation of K_2SO_4, K_2SO_3, K_2S, and K_2CO_3, it is clear that those predictions were based on poorly approximated data and on models that were too simplistic to be reliable (Ref. 1).

At the time this project began, the most direct progress on the seed-chemistry problem appeared to require the experimental determination of the vaporization thermodynamics of K_2S and K_2SO_3. A collaborative effort was mounted that included concurrent investigations at NASA-LeRC, the University of Toledo (UT), and Arkansas State University (ASU). Some of the results from this collaboration were published recently (Ref. 3). Much of the work done at ASU has not been reported, however, and comprises the bulk of this report.

1.2 PROGRAM OBJECTIVE AND PLAN

The objective of this program was to investigate the vaporization thermo-dynamics of K_2S and K_2SO_3, and to report any ancillary findings that might prove useful for MHD purposes. The program divided naturally into three tasks:

(1) Development of Experimental Facility

2

(2) K_2SO_3 Experiments

(3) K_2S Experiments

The Knudsen rate-of-effusion method (Ref. 4) was selected as the most direct method for obtaining vapor pressure data, and an experimental system was constructed for this purpose which provided microbalance capabilities at high temperatures under high vacuum. Since the vaporization reactions were unknown for both K_2SO_3 and K_2S, identification of species accompanying vaporization was of paramount importance. For this information we depended on the collaboration with LeRC referred to earlier. Other analyses and evaluations included vacuum tube furnace experiments, X-ray powder diffraction, thermal gravimetry, and chemical analyses and tests as appropriate.

Specific objectives included (for K_2SO_3 and K_2S):

(1) The vaporization reactions, i.e., the identification of products of vaporization.

(2) The temperature dependency of vapor pressures associated with the equilibrium vaporization reactions.

(3) The thermodynamic quantities accessible by combining the results of vapor pressure measurements with existing thermodynamic data.

With these results, it would be expected that a sophisticated equilibrium calculation, such as the NASA CEP of Gordon and McBride (Ref. 5), could provide reliable predictions about the potassium-oxygen-sulfur interactions in the MHD stream.

3

2. EXPERIMENTAL

2.1 HIGH TEMPERATURE VACUUM FURNACE AND VACUUM MICROBALANCE

All rate-of-effusion measurements were conducted in a modified Brew
Model 1068-C high temperature vacuum furnace, which utilized resistance
heating of tungsten mesh elements to provide a cylindrical hot zone of
2 in. dia. by 8 in. high. The 32 KVA power supply was designed to drive
the heating element to a maximum temperature of $3000^{\circ}C$. Tungsten radi-
ation shields (7 layers) surrounding the heating elements utilized a
"clam shell" design for ease of installing and removing specimens. Half
of the heater shell and tungsten shield assembly were mounted on a hinged
door of the vacuum vessel, providing easy access to the specimen when the
door was opened. The door included double "O" ring seals, with pumping
of the space between the "O" rings. It also included a one in. dia.
optically flat sight glass with an externally operated shutter to permit
line-of-sight optical pyrometer viewing of the center of the hot zone.
A series of 0.25 in. dia. holes in the radiation shielding provided the
optical path to the hot zone. A second, similar series of holes located
diametrically opposite the pyrometer sight path permitted thermocouple
access to the center of the hot zone. A water-cooled internal copper
heater shell (nickel flashed) and a double-wall, water-cooled stainless
steel external chamber assured a true cold-wall furnace with minimum heat
radiation to surrounding areas. Conventional vacuum feel-throughs were
employed. The pump stack was also conventional, consisting of an oil
diffusion pump, mechanical fore-pump, liquid nitrogen trap, and gate valve.
Typical pressures at temperature were in the 10^{-6} torr range without
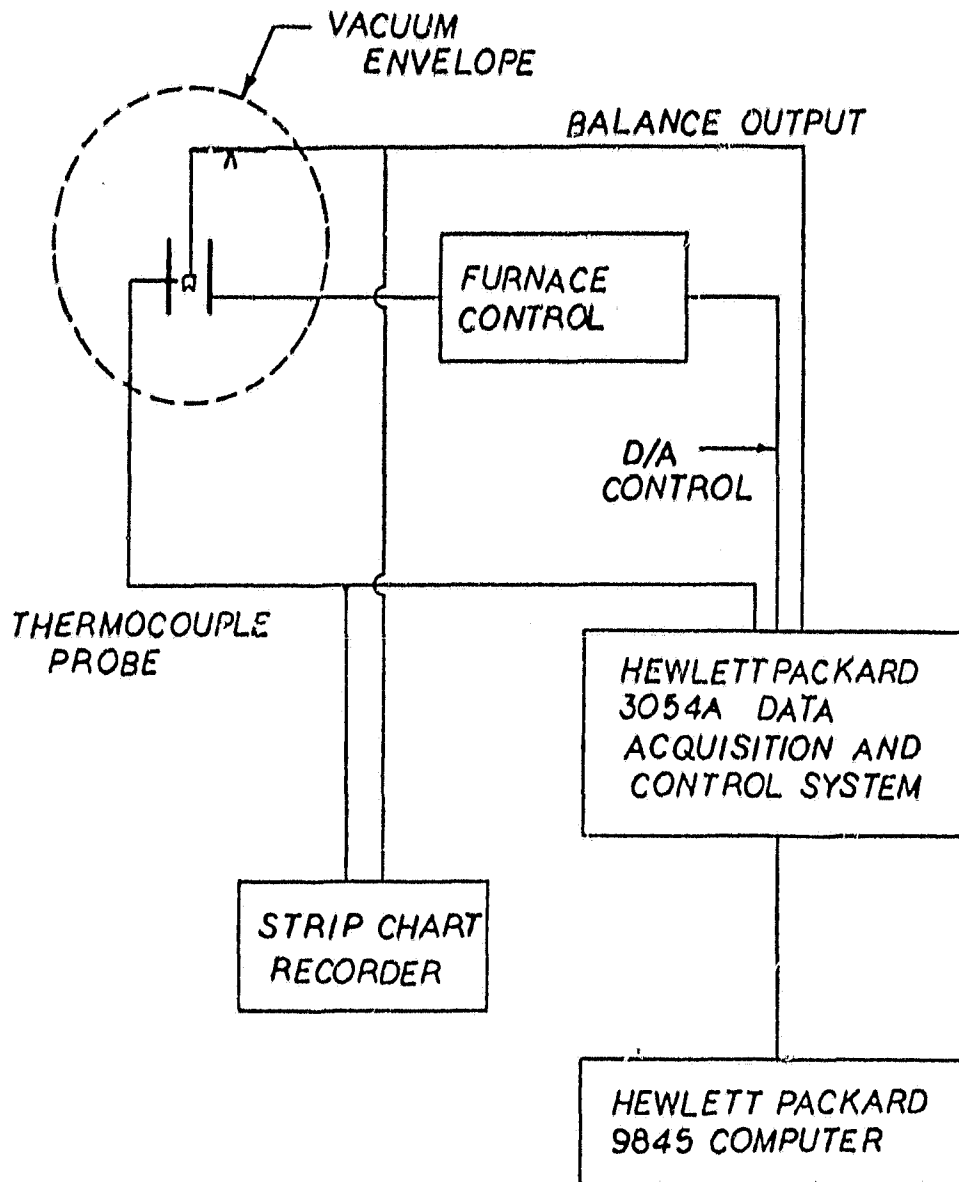
Figure 1. Schematic Diagram of Experimental System.

using liquid nitrogen.

A Cahn RG vacuum recording electromicrobalance was mounted on top of the furnace chamber so that the balance work load was suspended along the vertical axis of the hot zone. The glass vacuum chamber of the microbalance was joined to the stainless steel furnace chamber by a glass-to-metal seal which then permitted the use of standard high vacuum flanges. Access to the balance was through one end of the glass vessel which was equipped with a ground glass flange sealed by a metal plate with "O" ring. The balance was isolated from the hot zone and operated at room temperature. Work loads were suspended from the balance into the hot zone by means of tungsten or molybdendum hangdown wires which ranged in diameter from 0.05 mm to 0.125 mm. The hangdown wires passed through a series of 0.25 in. dia. holes in the radiation shielding. The distance from the balance beam to the center of the hot zone was about 20 in.

2.1.1 Thermocouple Calibration

A chromel-alumel thermocouple of 0.010 in. dia. wires in a 2-hole alumina sheath was located such that its bare junction was within about 0.25 in. of the sample-containing cell at the center of the hot zone. The thermocouple was calibrated with the aid of the microbalance in the following manner. A cylindrical graphite cell, suspended from the microbalance and typical of the cells used in the effusion experiments (Fig. 2), was equipped with small "fall-out" holes in its bottom. Small wedges (10 to 50 mg) of various high purity metals were fitted into the holes so that when they melted, they would fall from the cell and cause a sudden

6

displacement in the balance output. A two-pen strip chart recorder that monitored the balance and the thermocouple provided a convenient record of the apparent temperature at which fall-out occurred. Metals, their melting points, and correction's included:

Indium, 156°C (+40° correction)

Cadmium, 321°C

Lead, 327°C

Zinc, 419°C

Aluminum, 660°C (no corrections)

Silver, 961°C (no correction)

Several variations of this procedure were used, including attaching the small metal samples to hooks on the outside of the cell and using inert weights which were held to the cell by strips of the different metals and which fell when the strips melted. The main difficulty, which necessitated many repetitions, was due to unpredictable sticking of the metals (especially zinc) to the graphite cell on melting. As shown above, thermocouple corrections were unnecessary above the melting point of aluminum. Corrections below about 660°C were determined graphically from a curve established by repetitions of the fall-out procedure.

2.1.2 Data Acquisition and Control System

A Hewlett-Packard 9845 computer with a 3054A Automatic Data Acquisition/ Control System was used to control the furnace temperature and to monitor both the temperature and the microbalance. Digital to analog routines and hard-wire connections to the solid state controller of the furnace

permitted temperature control to within 1° at any operating temperature. The thermocouple described above was used to measure the temperature, and continuous computer interaction provided control signals to seek a zero difference between the thermocouple output and the set-point. Data acquisition via analog to digital routines included the thermocouple output, the microbalance output, and the time derivative of the balance output. These three quantities were also monitored continuously on a three-pen strip chart recorder. In fact, except for the temperature control, all data was read from the recorder chart, which proved to be more convenient than the computer-acquired data. Fig. 1 shows schematically the experimental system with the data acquisition/control system.

2.1.3 Knudsen Cells and Cell Materials

Table 1 summarizes results for materials used as containers for K_2SO_3 and K_2S under vacuum at high temperatures. No really good container material was found. The best appears to be high density graphite coated with pyrolytic graphite, though there is evidence that this material reacts with K_2SO_3 in an indirect manner (see section 2.2.3).

The Knudsen cells were simple in design (Fig. 2). The main design consideration was the total load capacity of the Cahn RG microbalance, which required that the sum of the Knudsen cell, hangdown wire, and sample be kept below 2 g. Other design considerations were to keep the orifice diameters small to assure that the effusing vapors were representative of equilibrium vaporization, and to avoid thick cell walls and thus avoid the need for corrections due to the impeding of molecular flow by the

8
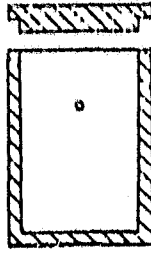
A. Cylindrical Cell with
   Orifice in Cell Side

B. Electron Beam Welded
   with Orifice in Top
   (Used for Pt, W)
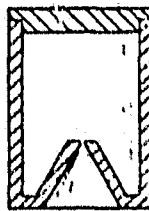
1 cm

C. Inverted Conical Orifice
   (Effusion from Bottom)

Figure 2. Knudsen Cell Designs.

Table I

Evaluation of Materials as Knudsen Cells for Containing

K_2S/K_2SO_3 in Vacuum at High Temperatures

Material	Observed Behavior	Evaluation
Pt	Yellow-brown discoloration of platinum above 800^oC. Not a large effect, but definite. No mass gain or loss of Pt observed. Erratic effusion results with K_2S.	Probably unsuitable for extended use above 800^oC.
Mo	Extensive reaction above 800^oC	Unsuitable
W	Extensive reaction above 800^oC	Unsuitable
Quartz	Becomes frosted, definite reaction above 800^oC	Unsuitable
Machinable Glass	Becomes frosted, definite reaction above 800^oC	Unsuitable
Boron Nitride	Initial bleached appearance where in contact with sample. Becomes eroded on extensive heating. Cell mass loss observed.	Unsuitable for extensive use.
Graphite, 1.81 g/cm^3	No reaction observed with K_2S. After extensive heating with K_2SO_3, erosion of cell observed. Evidence for mass loss with K_2SO_3.	Probably suitable for K_2S. Questionable for K_2SO_3. Perhaps porous to K vapors.

10

Table I (cont'd)

Material	Observed Behavior	Evaluation
Graphite, pyrolytic coated	No reaction observed with K_2S after extensive use. Becomes eroded after extensive use with K_2SO_3. Evidence for mass loss with K_2SO_3.	Probably suitable for K_2S. Questionable for K_2SO_3.
Alumina	No evidence of chemical reaction to 1300 C. No mass loss or gain observed. Erratic effusion results with K_2S--possible surface wetting effects.	Chemically inert. Possible surface wetting effects.

11

orifice channel (Ref. 4). No special significance is attached to the location of the orifice, which was determined by the ease of working with the cell material. For example, two platinum cells obtained from LeRC were electron beam welded and were constructed more conveniently by having the orifice in the top.

2.1.4 System Verification--The Vapor Pressure of Silver

A check against possible inductive interactions between the current flowing to the heating elements and the Knudsen cell suspended from the microbalance was obtained by rate-of-effusion measurements for silver, with subsequent vapor pressure calculations. This procedure was carried out several times during the project. Typical results in Table II and Fig. 3 show acceptable agreement with the critical values of Hultgren (Ref. 6). The slope of the plotted data yields an enthalpy of vaporization of 68.3±0.4 kcal/mol as compared with Hultgren's value for $\Delta H^{\circ}(298)$ of 67.900±0.200 kcal/mol.

The calculation procedure for Ag vapor pressures from rate-of-effusion data is illustrative of that for $K_2S_2O_5$, K_2SO_3, K_2S, to be discussed later. The Knudsen equation (Ref. 4) for the vapor pressure P in terms of rate-of-effusion is

$$P = \frac{\dot{\omega}}{AW}\sqrt{\frac{2\pi RT}{M}} \tag{1}$$

where $\dot{\omega}$ = mass effusing per second from the cell orifice

A = cross-section area of effusion orifice

W = correction factor for orifice (unity for all cells

   in this work).

Table II

Rate of Effusion and Vapor Pressures for Silver

#	10^9 x Rate, kg/s	°K	10^5 x P,atm
1	9.40	1489	14.1
2	5.26	1445	7.77
3	3.29	1417	4.81
4	1.39	1364	1.99
5	1.09	1349	1.55
6	1.28	1357	1.83
7	5.54	1308	0.778
8	0.271	1282	0.377
9	0.700	1323	0.989
10	0.242	1266	0.334
11	0.200	1269	0.277
12	0.232	1282	0.323
13	0.355	1305	0.498
14	0.496	1323	0.700
15	0.614	1331	0.870
16	0.714	1344	1.02
17	2.23	1403	3.24
18	3.72	1434	5.47
19	3.47	1423	5.08
20	8.98	1481	13.4
21	8.85	.1471	13.2

Table II (cont'd)

#	10^9 x Rate, kg/s	°K	10^5 x P,atm
22	1.88	1260	0.259
23	0.257	1266	0.355
24	0.279	1272	0.386
25	0.308	1276	0.427
26	0.290	1274	0.402
27	3.92	1410	5.71
28	0.442	1274	0.612
29	1.85	1376	2.66
30	2.53	1381	3.65
31	0.170	1260	0.234

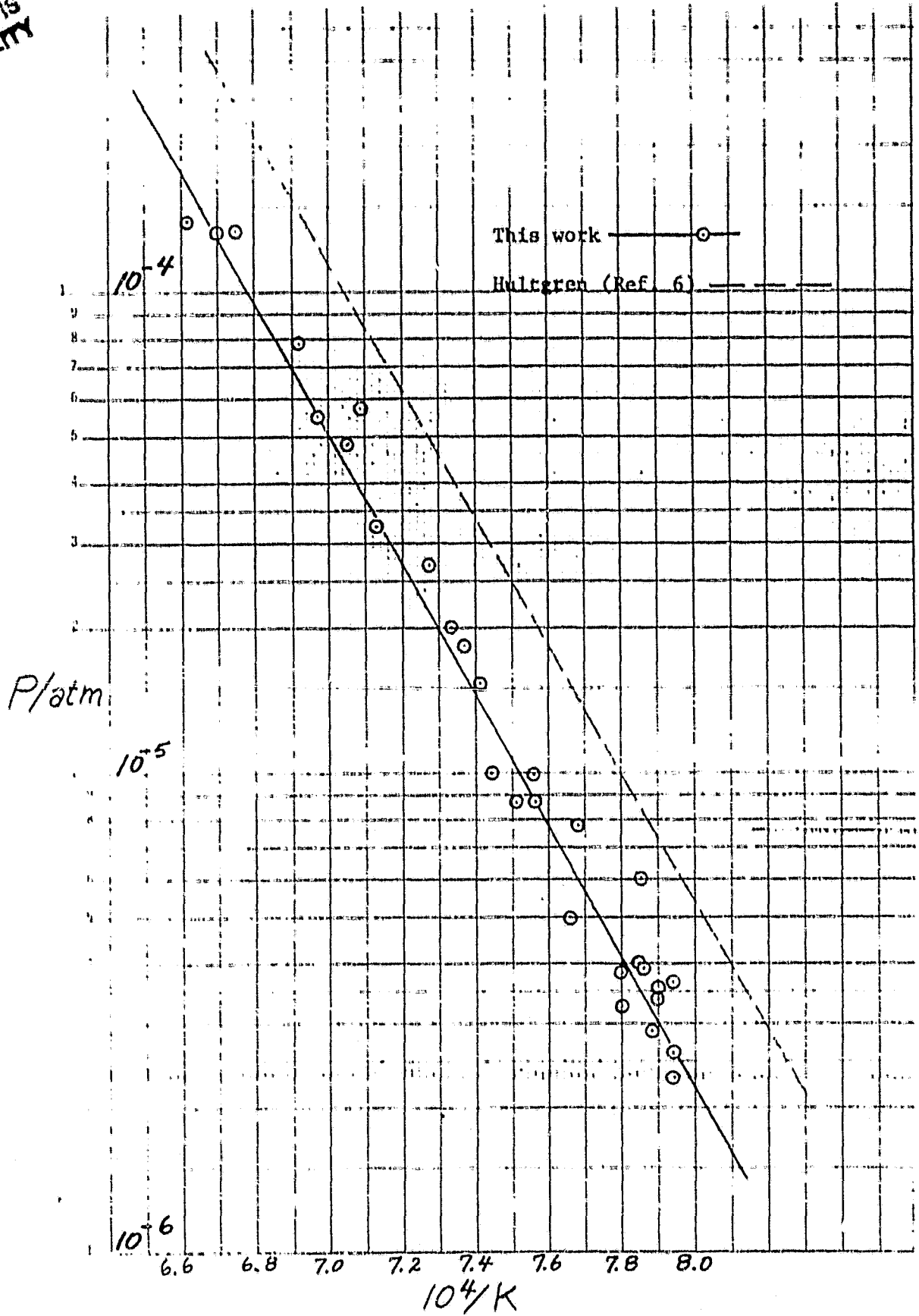Graphite Cell, Orifice Area $5.595 \times 10^{-7} M^2$

Figure 3. Log P(atm) vs 10^4/T for Silver in Graphite Knudsen Cell.

15

R = universal gas content

T = Kelvin temperature

M = molecular weight of effusing species

2.2 EXPERIMENTAL RESULTS FOR K_2SO_3

2.2.1 K_2SO_3 from the Thermal Decomposition of $K_2S_2O_5$

We reported previously (Ref. 3) the apparent contamination of commercial K_2SO_3 with K_2CO_3 and H_2O, and the confusion in the literature on whether commonly available "potassium sulfite" is K_2SO_3 or $K_2SO_3 \cdot 2H_2O$ (JCPDS Card No. 1-0895). To avoid these uncertainties, $K_2SO_3(s)$ was prepared by decomposition in vacuum of Fisher Reagent Grade potassium metabisulfite, $K_2S_2O_5$:

$$K_2S_2O_5(s) \xrightarrow{40-400^{o}C} K_2SO_3(s) + SO_2(g) \qquad (2)$$
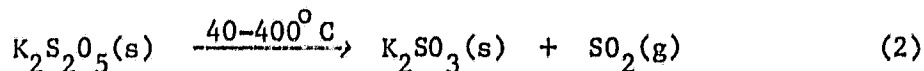
Well-defined K_2SO_3 was prepared by this method directly in the Knudsen cell at temperatures below 400 C. Subsequent K_2SO_3 studies were then conducted at higher temperatures ($\sim 700-1200^{o}C$) without breaking vacuum. The validity of reaction (2) was established by mass spectrometry at LeRC which showed $SO_2(g)$ as the only gaseous species, and by X-ray diffraction analyses at UT and ASU which showed the residue to be K_2SO_3. Thermogravimetric confirmation was also obtained. The theoretical yield of $SO_2(g)$ is 28.81% of the original $K_2S_2O_5$ according to decomposition following (2). Gravimetric determinations which involved various reaction temperatures, rates of heating, sample sizes, and container materials, were consistently near 28.81% in yield. At a fixed temperature, the loss

16

Table III

Rate of Effusion and Vapor Pressures for the
Reaction: $K_2S_2O_5 = K_2SO_3(s) + SO_2(g)$
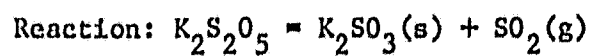
#	10^{10} x Rate, kg/s	°K	10^6 x P, atm
1	0.104	365	0.326
2	2.95	395	9.61
3	7.86	405	25.9
4	17.9	415	59.8
5	44.4	425	150.
6	7.11	405	23.5
7	19.2	415	64.1
8	42.2	425	143.
9	1.05	385	3.38
10	2.97	395	9.67

Graphite Knudsen Cell, Orifice Area $1.72 \times 10^{-7} M^2$
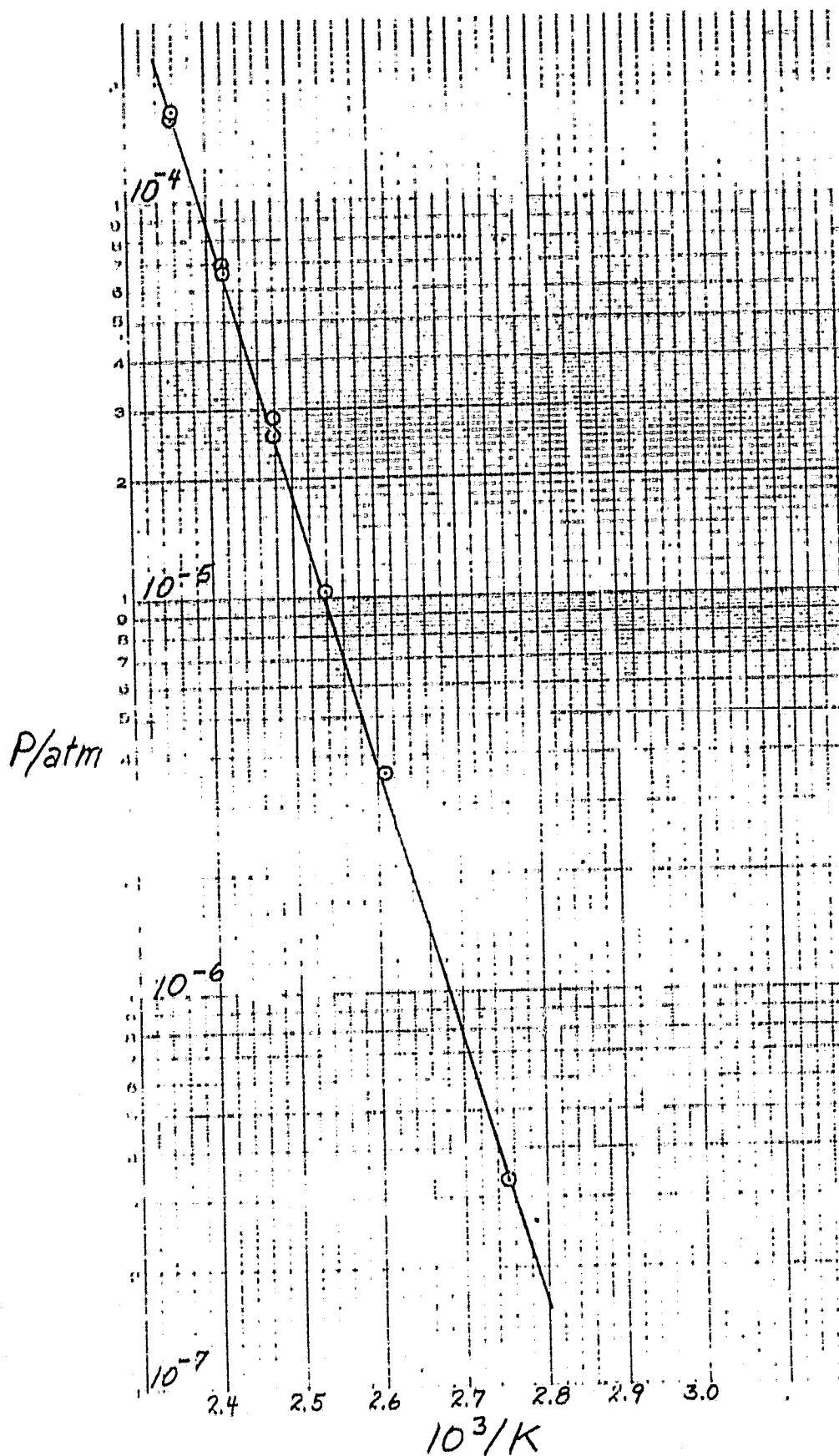
Figure 4. Log P(atm) vs $10^3/T$ for the Decomposition for $K_2S_2O_5$

of $SO_2(g)$ vs time gave a curve typically with a definite inflection point which always occurred at about the 50% depletion point of available SO_2. Constant rates of effusion were found to be impossible to attain once the 50% depletion point was reached for a given sample. Instead, the rates would fall off asymtotically. The effusion data in Table III were accordingly taken before the decomposition reaction was 50% complete. The pressures plotted in Fig. 4 yield a least squares fit for log P(atm) = $A + B/T$ of $A = 12.22\pm0.20$ and $B = -6816\pm100$.

2.2.2 K_2SO_3 Tube Furnace Studies

Preliminary mass spectrometric data obtained at LeRC on vapors above $K_2SO_3(s)$ was interpreted in terms of the reaction

$$2K_2SO_3(s) \longrightarrow K_2SO_4(s) + SO_2(g) + 2K(g) \qquad (3)$$
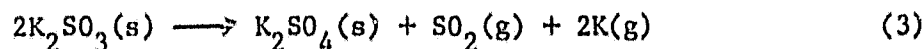
Early in this work, however, it became obvious that various sulfides of potassium, in addition to elemental sulfur, were produced when K_2SO_3 was vaporized. Initial studies were conducted in graphite cells and so the possibility was pursued that reduction by graphite was the source of the sulfur and sulfides. Subsequent results using cells of boron nitride, platinum, and alumina showed that potassium sulfides and elemental sulfur are unavoidable major products from the vaporization of $K_2SO_3(s)$, and not the result of a reduction reaction with the container. Since reaction (3) did not explain the vaporization of $K_2SO_3(s)$, a lengthy series of tube furnace experiments was conducted to characterize the condensates and residues from the reaction. These experiments utilized a simple vacuum manifold with a protruding Vycor tube over which an external tube furnace

(mounted on casters) could be positioned. After completion of an experiment, the furnace was rolled back, permitting removal of the Vycor tube (containing the sample) in a glove bag filled with dry nitrogen. Results from the tube furnace studies include:

(1) K_2SO_4, K_2S_3, K_2S_5, and additional unidentified sulfides were obtained in the cell residues.

(2) S_2, K, and unidentified sulfides were obtained as condensates.

(3) A test for SO_2(g) as a major product of vaporization of K_2SO_3 was negative.

(4) Results 1-3 are intrinsic to K_2SO_3 and not due to reaction with container materials.

2.2.3 Thermal Gravimetric Analysis (TGA) of K_2SO_3

Samples of $K_2S_2O_5$ were subjected to vaporization in vacuum in which the temperature was driven up at a constant rate. The purpose was to establish the various plateaus in the TGA weight loss curve and thereby identify the successive reaction products. Fig. 5, which is a typical result using a platinum cell, shows the regions of volatility for $K_2S_2O_5$, K_2SO_3, and K_2SO_4, respectively. In the following reaction series, for which all masses are relative to 100% for the original $K_2S_2O_5$, the TGA plot should show successive losses of 28.8%, 32.0%, and 39.2%.

$$K_2S_2O_5(s) \ = \ K_2SO_3(s) \ + \ SO_2(g) \qquad\qquad (4)$$

100%   71.2%   28.8%

$$2K_2SO_3(s) \ = \ K_2SO_4(s) \ + \ 2K(g) \ + \ SO_2(g) \qquad (5)$$

71.2%   39.2%   32.0%

A. $K_2S_2O_{5(s)} \longrightarrow K_2SO_{3(s)} + SO_{2(g)}$
B. VAPORIZATION OF K_2SO_3
C. VAPORIZATION OF K_2SO_4
D. VAP. RATE INCREASE DUE TO TEMP. INCREASE
E. DEPLETION OF SAMPLE ~ 100%
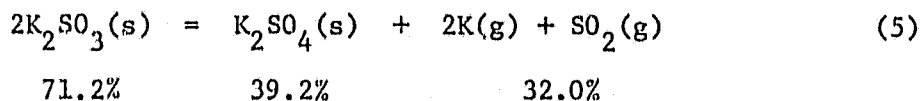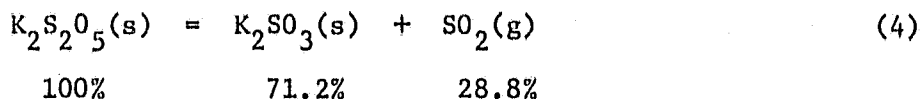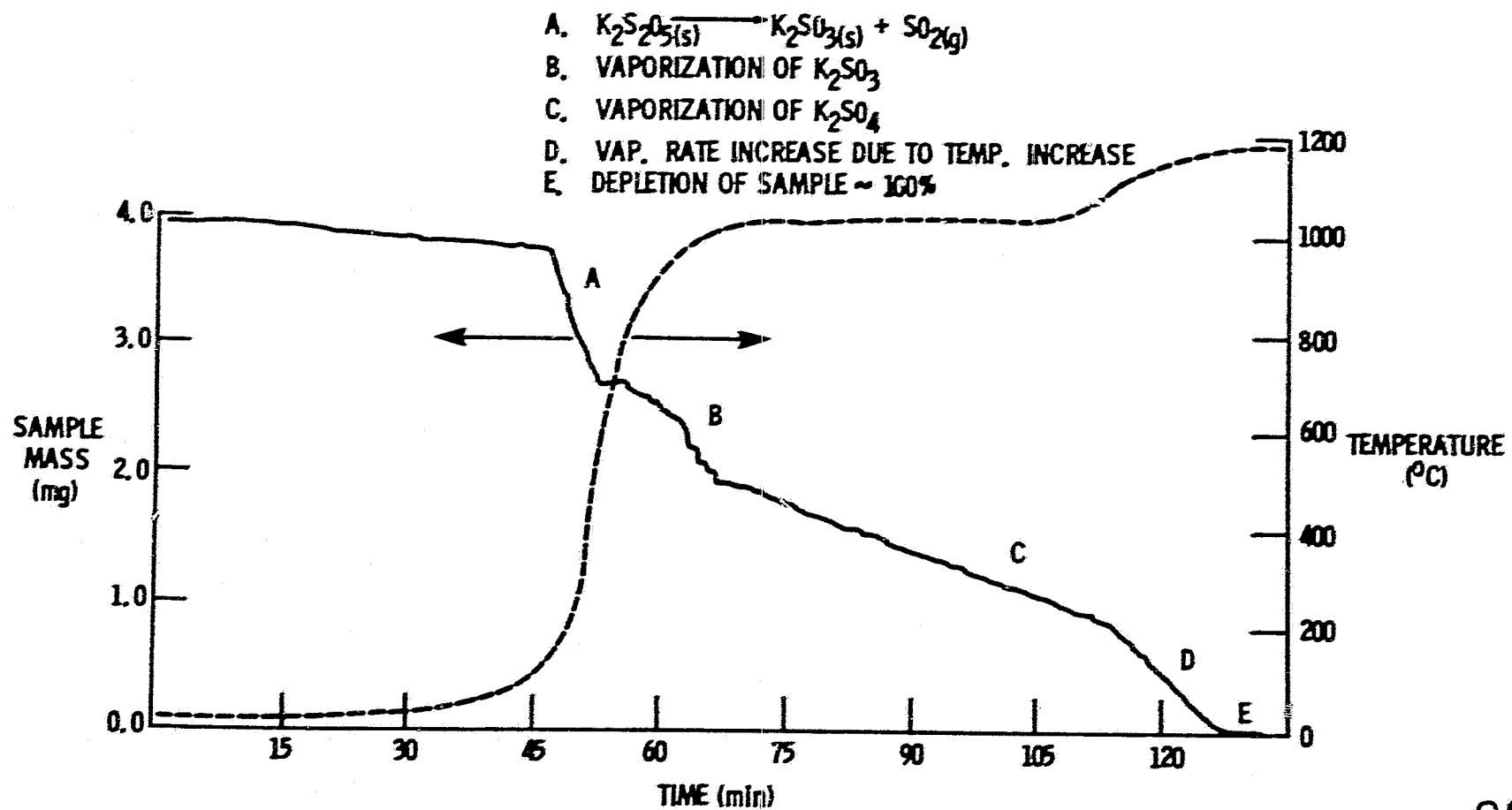
Figure 5. Thermogravimetric Analysis for $K_2S_2O_5$--K_2SO_3--K_2SO_4.

$$K_2SO_4(c) = K_2SO_4(g) \qquad\qquad (6)$$

$$\text{39.2\%} \qquad\quad \text{39.2\%}$$

There is no question about the correctness of reaction (4), as discussed earlier and as further evidenced by data of Table IV. Reaction (3), however, is not consistent with the TGA data. None of the results in column 2 of Table IV corresponds to the required value of 32.0%. In fact, no one reaction has been proposed that will account for the TGA data of K_2SO_3. On the basis of the tube furnace results, and mass spectrometric results of the next section, a plausible reaction is

$$4K_2SO_3(s) = 3K_2SO_4(s) + K_2S(g) \qquad\qquad (7)$$

$$\text{71.2\%} \qquad\quad \text{58.8\%} \qquad\quad \text{12.4\%}$$
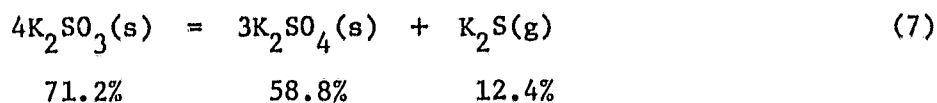
where the percentages are again in terms of the original $K_2S_2O_5$. Reaction (7), with parallel contributions from (5) provides a consistent account of results with Pt containers. The TGA curves obtained using BN cells and graphite cells exhibited no plateau corresponding to the depletion of K_2SO_3 to leave just K_2SO_4. Reaction with the cell is indicated. In the BN results of Table IV, mass loss was greater than 100% of the original $K_2S_2O_5$. The graphite cell results show losses of 107 and 99%. It is important to realize that the BN and graphite experiments did not involve temperatures high enough to cause vaporization of K_2SO_4 (first discernible in our system and cells at about 1025°C). It should be further noted that in experiments which were interrupted before sample depletion, X-ray diffraction of the residue always showed K_2SO_4 to be present. Thus while K_2SO_4 is formed, it is also consumed, implying that the cell reaction (for both BN and graphite cells) is between the cell and K_2SO_4, not the cell and K_2SO_3. The fact that all of the K_2SO_3 and all of the K_2SO_4 eventually

22

disappear requires that one of the products from the reaction between K_2SO_4 and the cell must be K_2SO_3. For the graphite cell, the most plausible reaction is

$$K_2SO_4(s) + 1/2 \ C(s) = K_2SO_3(s) + 1/2 \ CO_2(g) \qquad (8)$$
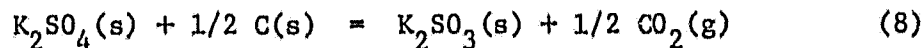
In this manner all the K_2SO_4 produced by reactions (5) and (7) would be consumed, and so would all of the K_2SO_3. A similar kind of cycle is believed to be involved for the BN cell, but since BN cells were abandoned, no attempts were made to identify the specific reactions.

The extent of graphite cell reaction can be predicted if the source of K_2SO_4 is considered to be from reaction (7), which when added to (8) yields the _formal_ net result

$$4K_2SO_3(s) = 3K_2SO_4(s) + K_2S(s) \qquad (7)$$

$$3K_2SO_4(s) + 3/2 \ C(s) = 3K_2SO_3(s) + 3/2 \ CO_2(g) \qquad (8)$$

$$\overline{K_2SO_3 + 3/2 \ C(s) = K_2S(s) + 3/2 \ CO_2(g)} \qquad (9)$$
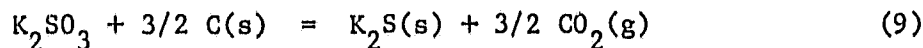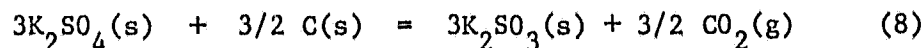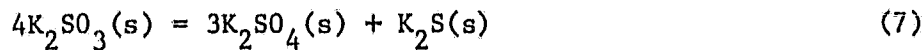
71.2%   8.1%   49.6%   29.7%

The mass loss to be expected from the total reaction sequence is 28.8% by SO_2 evolution from (4), 49.6% from vaporization of K_2S, and 29.7% from CO_2 evolution, for a total of 108.1% of the original $K_2S_2O_5$. Results in terms of actual cell loss should also be noted. From (9), a $K_2S_2O_5$ sample of 100 mg would cause 8.1 mg of the graphite cell to be lost. A typical cell weighed about 1500 mg, which means that in addition to sample loss, a change of 8.1/1500, or about 0.5%, in the cell mass must be detected in the course of an experiment. For experiments of heating duration from several hours to several days, it is easy for a 0.5% change in cell mass to be obscured by accumulative uncertainties. The indicated

Table IV

Thermogravimetric Analyses for $K_2S_2O_5$--K_2SO_3

| Expt #	% loss in forming K_2SO_3 from $K_2S_2O_5$ [1]	% loss after K_2SO_3 formed [2]	Container
1	28.8	18.9 (T<1000 C)	Pyrolytic graphite
2	28.3	17.6	Pt pan
3	27.8	16.6	Pt pan
4	29	----	Pt pan
5	28.8	26	Pt cell
6	28.8	25	Pt cell
7	28	25	Pt cell
8	28.5	88	BN cell
9	----	24	Pt cell
10	28.8	22	Pt cell
11	26.3	89	BN cell
12	28.5	23	Pt cell
13	28	79	Graphite
14	28.1	71	Graphite

[1] 28.8% theoretical

[2] At T below K_2SO_4 volatility

range of detectability is, however, well within microbalance capabilities, and the cell change can be detected, particularly now that reaction (8) has been revealed. For smaller samples (the smallest in any of the ASU experiments was 4.0 mg), gravimetric detection becomes proportionally more difficult. The 4.0 mg sample, for example, would involve a loss of about 0.02% of the graphite cell and would require detection over the duration of an experiment of 0.3 mg loss from a total of 1500 mg.

2.2.4 Mass Spectrum of Vapors Over K_2SO_3

Once it was established that elemental sulfur and mixed sulfides are produced when K_2SO_3(s) is vaporized under vacuum, further mass spectrometric measurements were carried out at LeRC (Ref. 3). The results (Fig. 6) are consistent with the tube furnace and TGA findings, but they are not definitive regarding the extent of reaction (5). Mass 64 could include contributions from both SO_2^+ and S_2^+, but because of the overall low intensities, isotopic peak measurements at mass 66 and 68 were inconclusive in resolving this question. The ratio of intensities for SO_2^+/ SO^+ was observed to increase with temperature, which would be expected if both SO_2 and S_2 contributed to m/e = 64. Parent species not involving SO^+ or SO_2^+ are believed to be K^+, S_2^+, K_2S^+, $K_2S_2^+$, $K_2S_3^+$, $K_2S_4^+$, and $K_2S_5^+$. The species KS^+ and KS_2^+ are probably fragment products. This interpretation agrees with the tube furnace and TGA results for reaction (7)

$$4K_2SO_3(c) = 3K_2SO_4(s) + K_2S(s/g) \qquad (7)$$
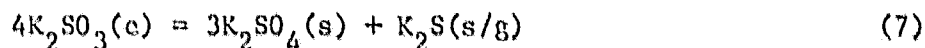
The K_2SO_4 (m.p. 1069°C) is not volatile at the temperature (760°C) of the mass spectrometric measurements and would not contribute any vapor species.
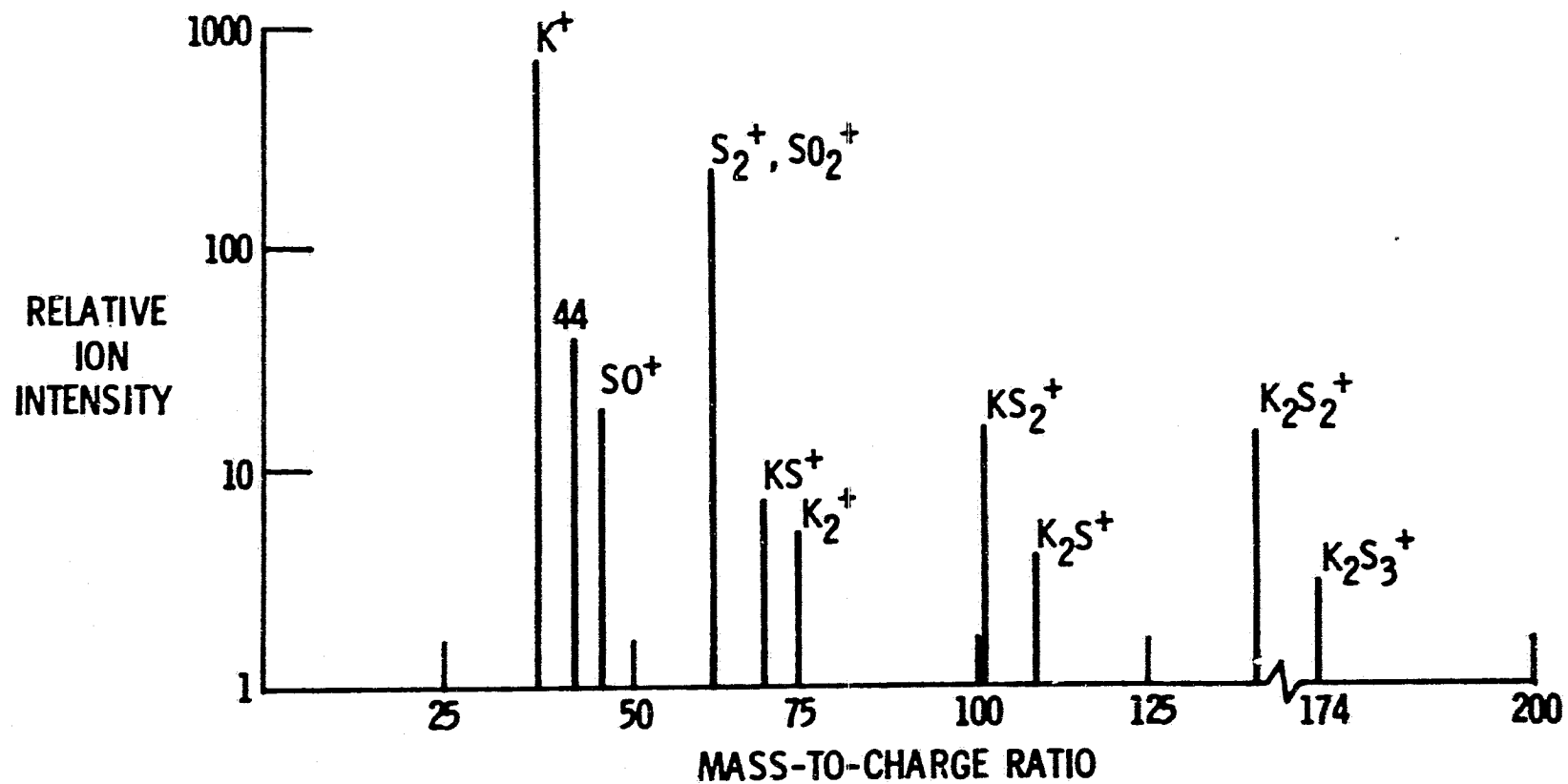
Figure 6. Mass Spectrum of Vapors from K_2SO_3.

The parent species listed above result from the subsequent vaporization of K_2S:

$$xK_2S(s) = (2x-2)K(g) + K_2S_x(c/g) \qquad (10)$$

$$K_2S_x(c/g) = 2K(g) + \frac{x}{2}S_2(g) \qquad (11)$$
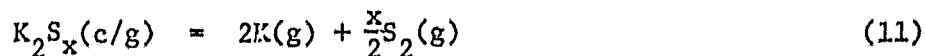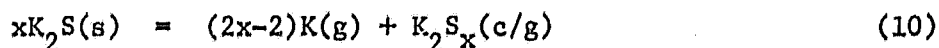
$$x = 1,2,3....$$

The peak at $m/e = 44$ is assigned to CO_2^+ as predicted by reaction (8). It is worth noting that the relative intensity at $m/e = 44$ is exceeded only by that of K^+ and S_2^+/SO_2^+.

2.2.5 Rate-of-effusion Results for K_2SO_3

2.2.5.1 K_2SO_3 Effusion from Boron Nitride Knudsen Cells

Because the TGA studies established that BN cells react with K_2SO_3, and because the nature of the reaction is unknown, little progress is possible with calculations based on effusion data from BN cells. Results are nevertheless reported for possible value to future studies. Pressures in Table V and Fig. 7 were calculated by assuming reaction (5) and ignoring the cell reaction. The effusion rates do not involve any assumptions, however, and constitute primary data for the K_2SO_3--BN system.

2.2.5.2 K_2SO_3 Effusion from Graphite Cells

Results for K_2SO_3 effusion from pyrolytic-graphite coated, high density (1.81 g/cm^3) graphite cells appear in Table VI. The data are tabulated in the order they were acquired and show an abrupt increase (see Fig. 8) in the effusion rate after "point" number 8, where a change from 2.02×10^{-10}

Table V

Rates-of-Effusion and Vapor Pressures for K_2SO_3
Vaporization from a Boron Nitride Knudsen Cell

T,°K	*Effusion Rate, kg s^{-1}	P,atm
1103	1.69×10^{-9}	3.57×10^{-5}
1093	1.38×10^{-9}	2.90×10^{-5}
1068	6.17×10^{-10}	1.28×10^{-5}
1148	8.24×10^{-9}	1.77×10^{-4}
1081	8.67×10^{-10}	1.81×10^{-5}
1048	3.00×10^{-10}	6.17×10^{-6}
1053	3.75×10^{-10}	7.73×10^{-6}
1061	3.92×10^{-10}	8.12×10^{-6}
1103	1.42×10^{-9}	3.00×10^{-5}
1108	1.81×10^{-9}	3.83×10^{-5}
1123	2.65×10^{-9}	5.64×10^{-5}
1139	5.52×10^{-9}	1.18×10^{-4}
1168	9.17×10^{-9}	1.99×10^{-4}
1153	6.35×10^{-9}	1.37×10^{-4}
1108	1.44×10^{-9}	3.05×10^{-5}
1113	1.68×10^{-9}	3.56×10^{-5}
1038	1.71×10^{-10}	3.50×10^{-6}
1028	9.17×10^{-11}	1.87×10^{-6}
1103	1.21×10^{-9}	2.55×10^{-5}

* Boron nitride cell with 0.813 mm dia orifice. Clausing factor taken
as unity. M in Knudsen eqtn. equals 0.04674 kg.
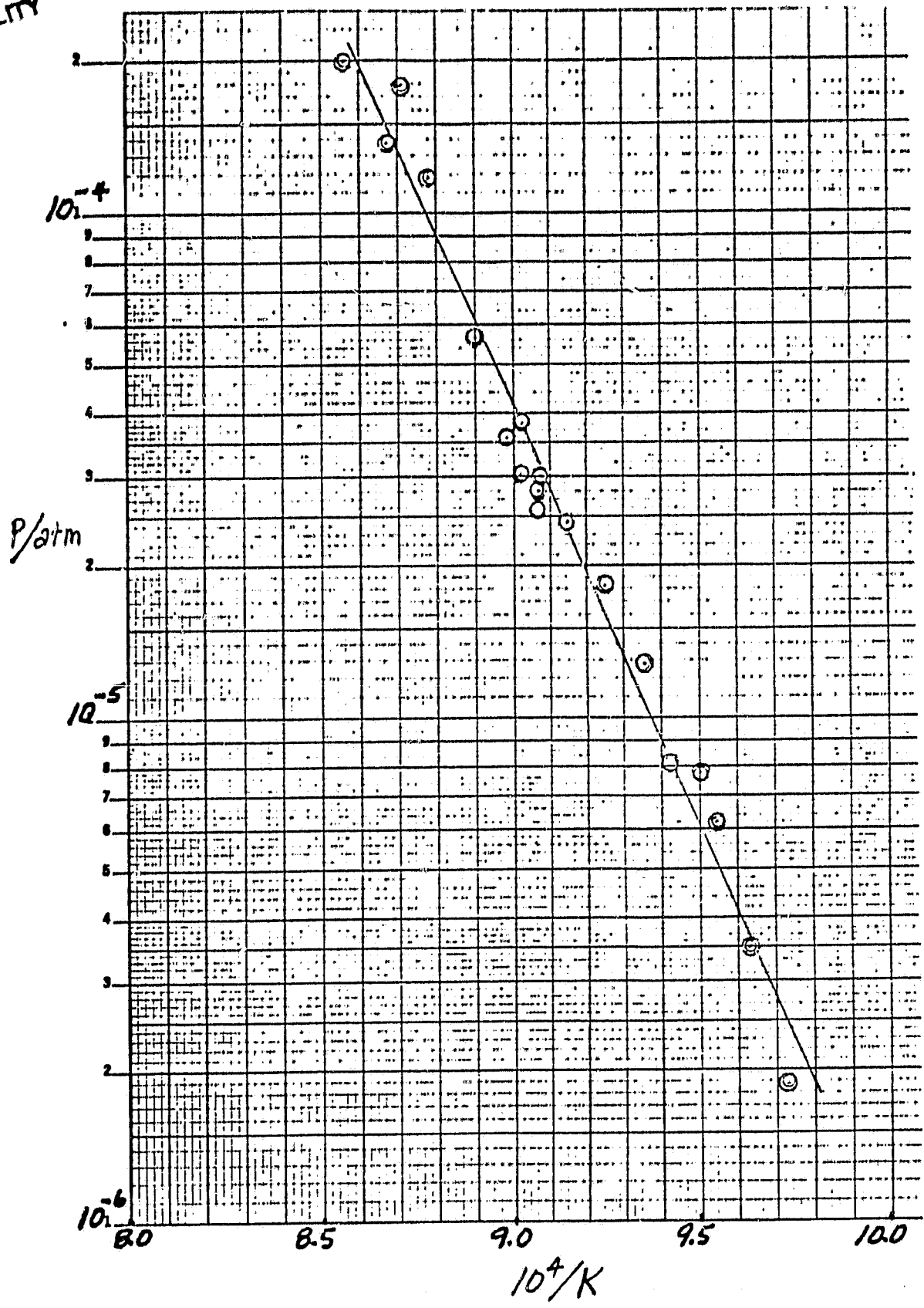
Figure 7. Log P(atm) vs $10^4/T$ for Vaporization of K_2SO_3 from Boron Nitride Knudsen Cell.

29

Table VI

Rates of Effusion and Vapor Pressures for K_2SO_3
Vaporization from a Graphite Knudsen Cell

#	10^{10} x Rate, kg/s	°K	10^6 x P, atm
1	0.444	1023	2.72
2	0.739	1048	4.59
3	1.23	1063	7.69
4	1.90	1093	12.1
5	1.15	1073	7.23
6	1.96	1093	12.4
7	2.41	1103	15.4
8	2.02	1098	12.8
9	4.45	1098	28.3
10	3.12	1093	19.8
11	5.25	1103	33.5
12	5.97	1113	38.2
13	8.21	1123	52.8
14	8.12	1133	52.4
15	9.48	1143	61.5
16	11.2	1153	73.0
17	2.43	1073	15.3
18	4.61	1113	29.5
19	7.13	1133	46.0
20	11.6	1153	75.6

Table VI (cont'd)

#	10^{10} x Rate, kg/s	°K	10^6 x P,atm
21	14.0	1163	91.6
22	17.4	1173	114.
23	21.7	1183	143.
24	5.70	1113	36.5
25	21.7	1183	143.
26	28.5	1193	189.
27	2.22	1073	14.0
28	2.69	1083	17.0
29	3.40	1093	21.6
30	4.49	1098	28.5
31	5.87	1108	37.5
32	7.63	1118	49.0
33	9.53	1128	61.4
34	12.0	1138	77.7
35	2.72	1073	17.1

Graphite Knudsen Cell, Orifice Area 1.72 x $10^{-7} M^2$
Points 1-8 apply to reaction (10).
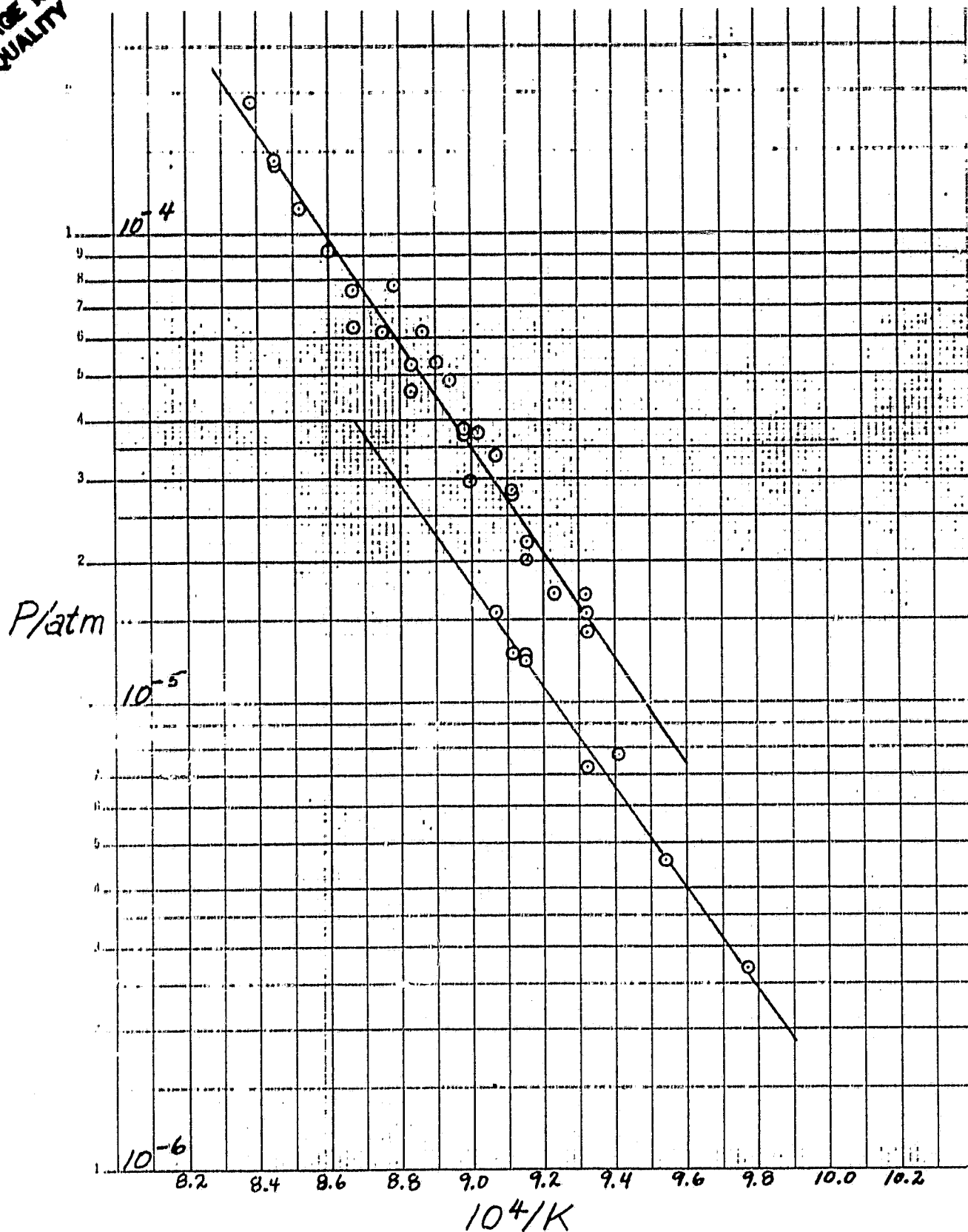Points 9-35 apply to reaction (11).

Figure 8.   Log P(atm) vs $10^4/T$ for Vaporization of K_2SO_3 in a Graphite
Knudsen Cell.

to 4.45×10^{-10} kg/s was observed. The first eight determinations are attributed to reaction (7) with the effusate consisting of products resulting from (10) and (11). The abrupt increase is due to the onset of the reaction of K_2SO_4 with the graphite cell and reflects the addition of $CO_2(g)$ to the vapors.

2.2.5.3 K_2SO_3 Effusion from Platinum Cells

Platinum cells, electron beam welded, with the effusion orifice in the top (Fig. 2), were loaded through the orifice with $K_2S_2O_5$. After thermal decomposition to form K_2SO_3, effusion data of Table VII were obtained. From earlier discussion, the predominant vaporization reaction for K_2SO_3 in platinum appears to be reaction (7). The calculated pressures are lower than those from BN or graphite cells as expected, but they are also much more eratic (Fig. 9). Reaction between the platinum cell and the sample was not extensive, as evidenced by the constant cell observed after total exhaustion of the sample. Experiments in open platinum pans revealed a brown discoloration of the platinum, but this was not accompanied by discernible mass gain or loss.

2.3 EXPERIMENTAL RESULTS FOR K_2S

2.3.1 K_2S Samples

Commercially available samples were found to be insufficiently well-defined for purposes of this work. They were unsatisfactory either in stated composition, such as the Alfa K_2S_x, S > 12.8%, used in our first

33

Table VII

Rates of Effusion and Vapor Pressures for K_2SO_3
Vaporization from a Platinum Knudsen Cell

#	10^{10} x Rate, kg/s	°K	10^6 x P,atm
1	2.01	1103	0.393
2	7.95	1195	1.62
3	6.49	1177	1.31
4	3.24	1165	0.651
5	2.24	1150	0.447
6	10.8	1285	2.28
7	4.82	1215	0.989
8	6.18	1225	1.27
9	1.45	1078	0.280
10	1.46	1085	0.283
11	1.71	1107	0.335
12	1.65	1134	0.327
13	1.85	1144	0.369
14	3.39	1167	0.682
15	5.77	1184	1.17
16	5.33	1189	1.08

Pt Knudsen Cell, Orifice Area 1.77 x $10^{-7} M^2$

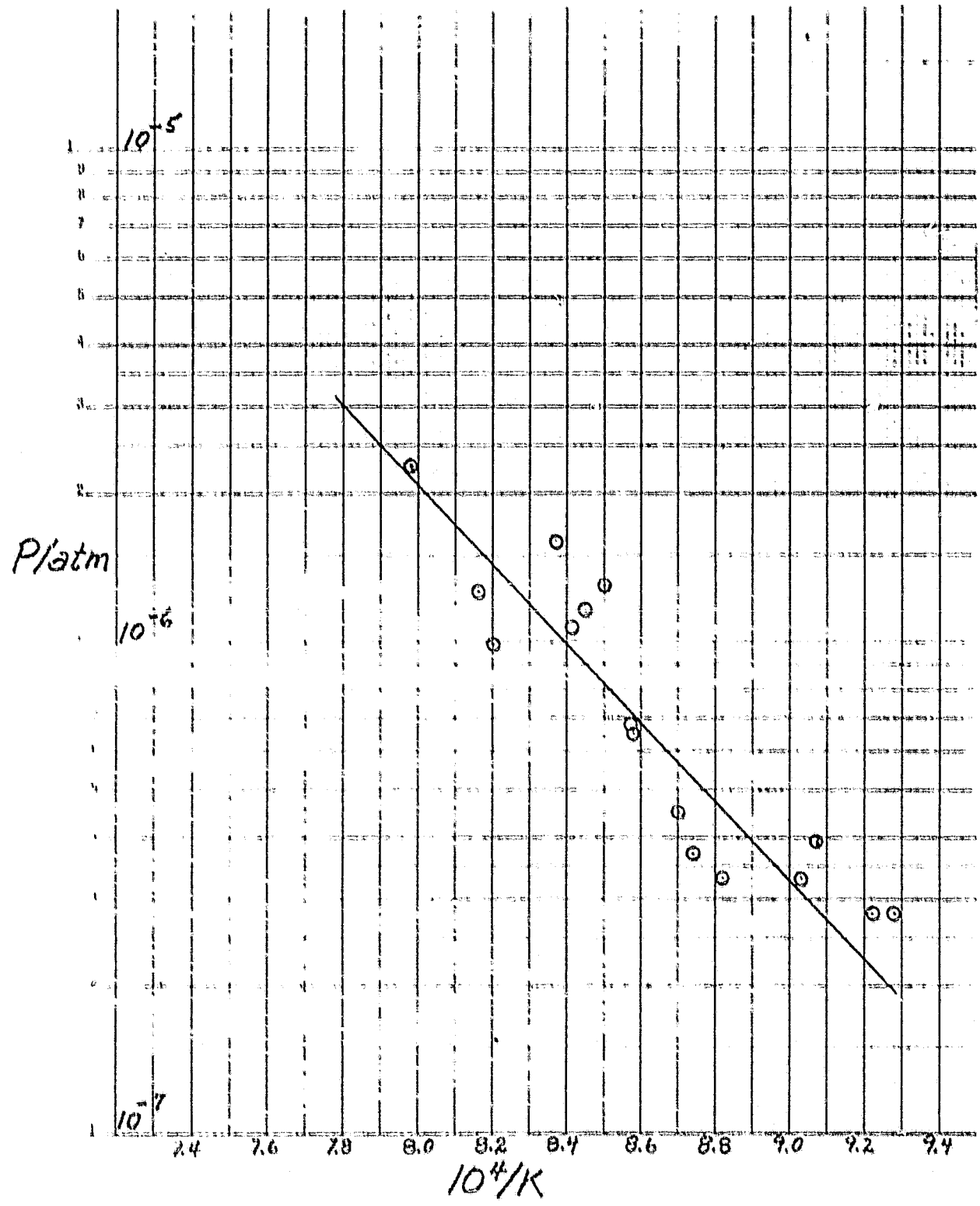Pressures apply to reactions (10) and (11)

Figure 9. Log P(atm) vs 10^4/T for Vaporization of K_2SO_3 in a Platinum Knudsen Cell.

study (Ref. 1), or they were of anomalously high volatility, as we found with samples obtained from Cerac. Suitable samples were synthesized directly from the elements (Ref. 8) in a dry box under argon by the group at UT. In their procedure, sulfur was added to a stoichiometric excess of potassium in a pyrex cup at 180° C. The metal-rich crude product was transferred under argon to a vacuum line where the excess potassium was sublimed at $350-400^{\circ}$ C. The product was analyzed by X-ray powder diffraction and by titration with standard acid. The X-ray diffraction pattern was that of K_2S (JCPDS Card No. 23-496A). The titration was interpreted as though the sample were K_xS_1 with a typical result of $x = 1.97 \pm 0.04$. Because K_2S reacts on contact with moisture from the air, subsequent handling and transferring of samples required either dry box or dessicator techniques.

2.3.2 Mass Spectrum of Vapors Over K_2S

Mass spectrometry at LeRC of the vapors from $K_2S(c)$ revealed the ionic species of Fig. 10 (Ref. 3), which are very similar to results of Ortman et al (Ref. 9). Parent species are believed to be K^+, S_2^+, K_2S^+, $K_2S_2^+$. Fragmentation species are KS^+ and KS_2^+. One would also predict K_2S_3, K_2S_4, K_2S_5, as vaporization products, though they were not detected unfragmented. As the vaporization proceeded, the ratios of the two most intense species, K^+ and S_2^+, were observed to change, with the relative intensity of K^+ decreasing smoothly, while that of S_2^+ increased (Fig. 11). Initially the ratio for K^+/S_2^+ was greater than 200, and after an extended period of heating at $>700^{\circ}$ C, the ratio finally became less than about 4 when the sample was almost completely gone. The results confirm the K_2S
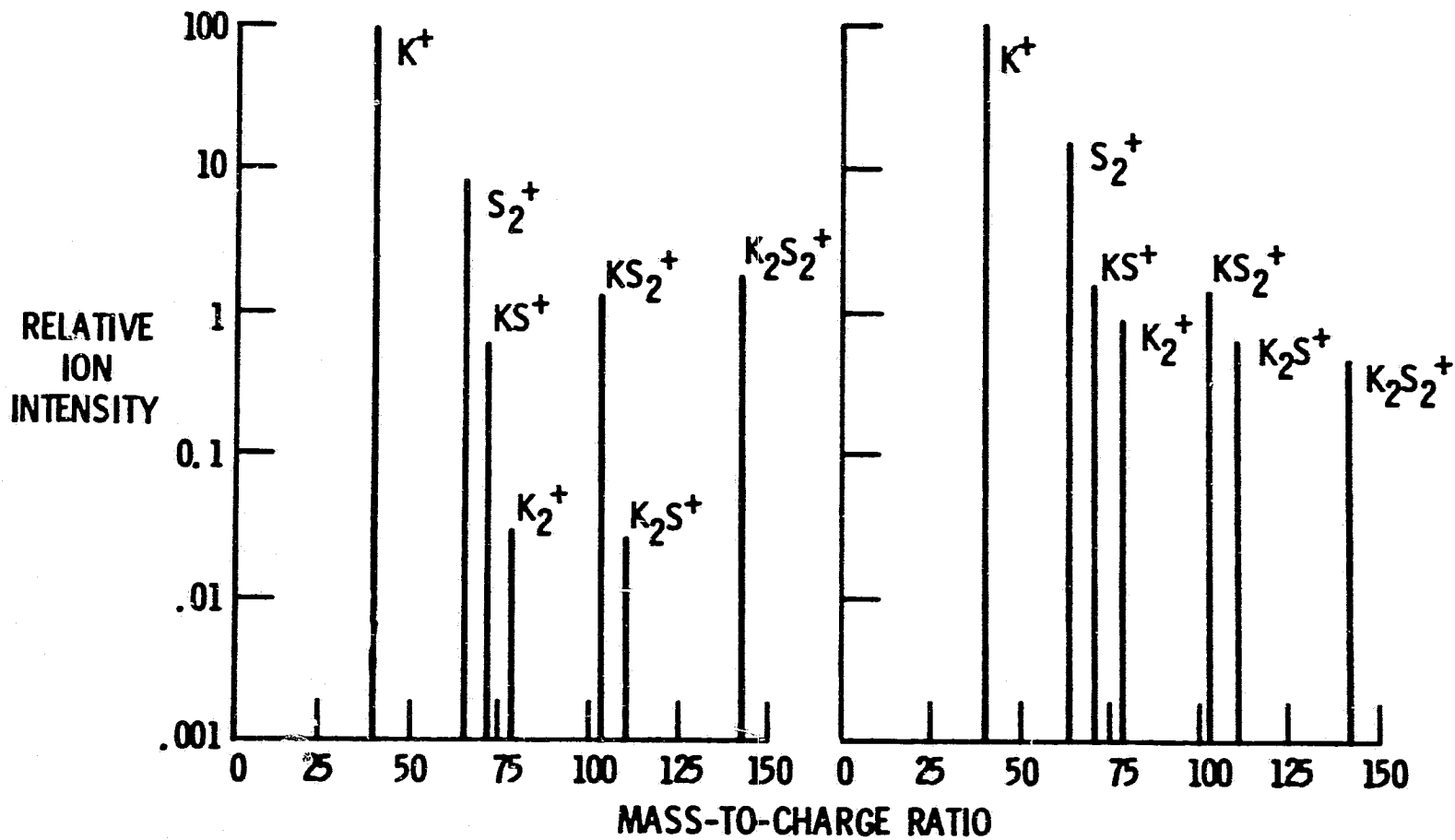
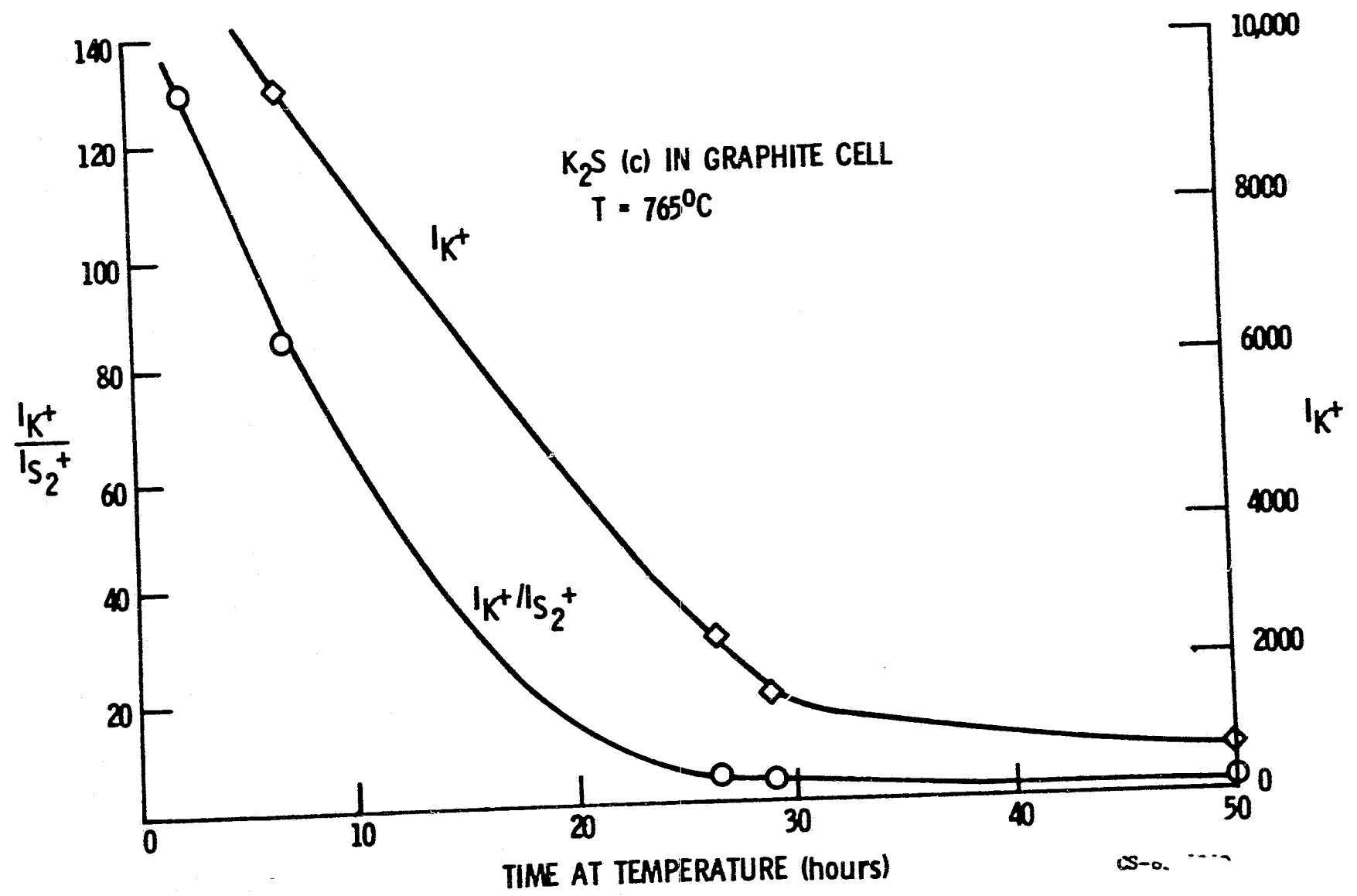Figure 10. Mass Spectrum of Vapors from K_2S.

Figure 11. Variation of Ion Intensities with Time.

vaporizes incongruently, as predicted by reaction (10).

2.3.3 Isothermal Total Mass Loss Experiments

Further characterization of the incongruent vaporization of K_2S was
sought from vacuum microbalance experiments in which K_2S samples (20-
100 mg) were vaporized isothermally. Evidence for incongruency from
such experiments is provided by departure from a horizontal line of the
curve from a plot of rate-of-effusion vs time. Alternatively, since
the temperature is constant, rate-of-effusion vs fraction of sample
vaporized should plot as a horizontal line for congruent vaporization,
and deviation from the horizontal would be evidence of incongruent vapori-
zation. Results for graphite and for alumina cells, Figs. 12 and 13
respectively, leave no doubt about the incongruent vaporization of K_2S.
The experiments were repeated several times, and though details of the
changes in rate were never identical from one experiment to the next,
certain features were nevertheless always present. The large maximum
exhibited by the rate was always observed, and it always occurred early
in the history of the sample in alumina cells, and late in the sample's
history in graphite cells. A sharp decrease always occurred after the
maximum, followed by more "regular" behavior. While these results
provide ample evidence of the incongruent vaporization of K_2S, they are
not understood. The early appearance of the maximum in alumina cells
caused alumina to be abandoned as a cell material, even though total
mass loss indicated no permanent change in the alumina. Subsequent
measurements were restricted to graphite Knudsen cells, and were made

40

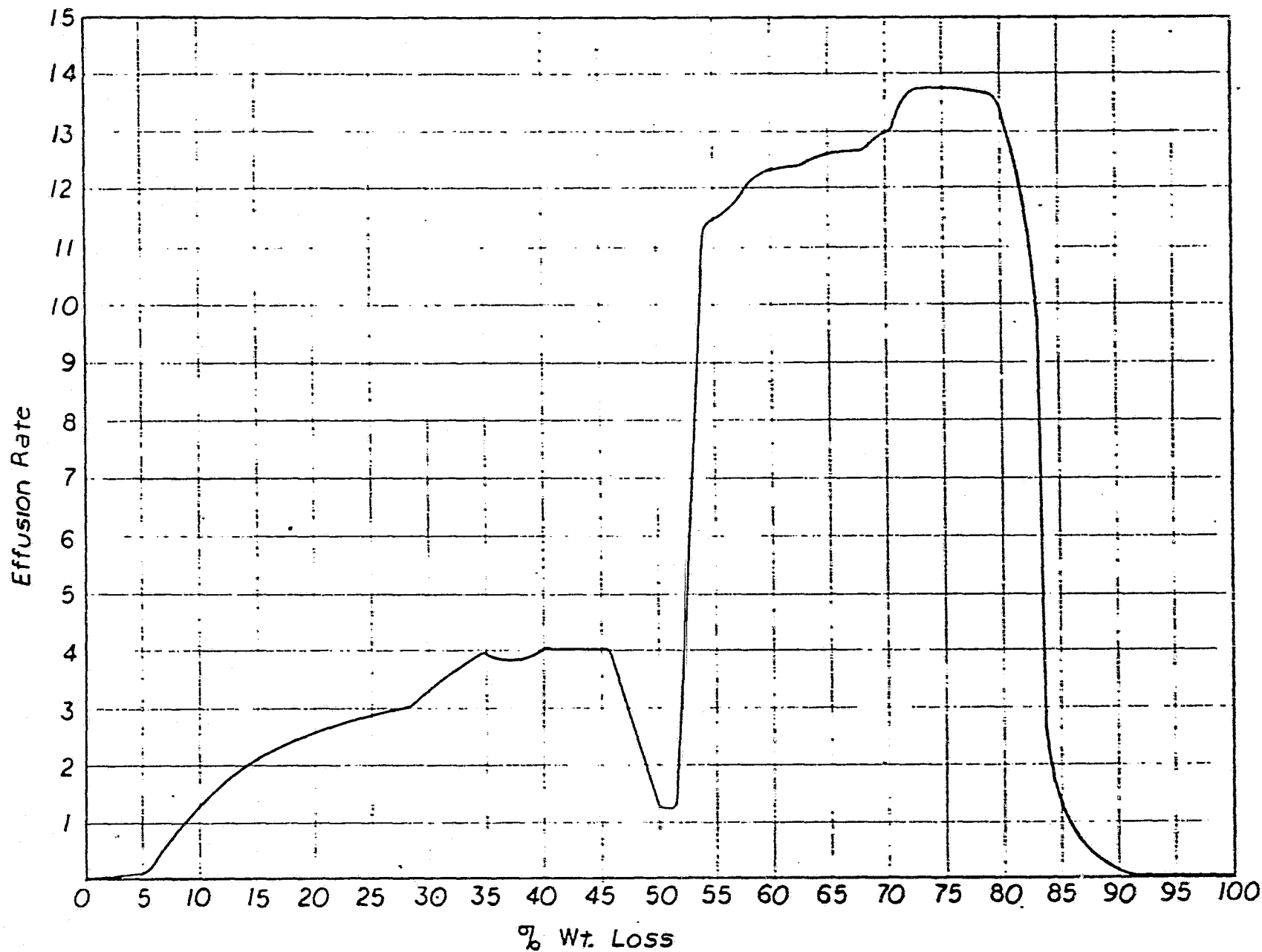Figure 12. Isothermal Rate-of-Effusion vs. Fraction Vaporized. K_2S at $780^{\circ}C$ in Graphite Cell. Rates are relative.
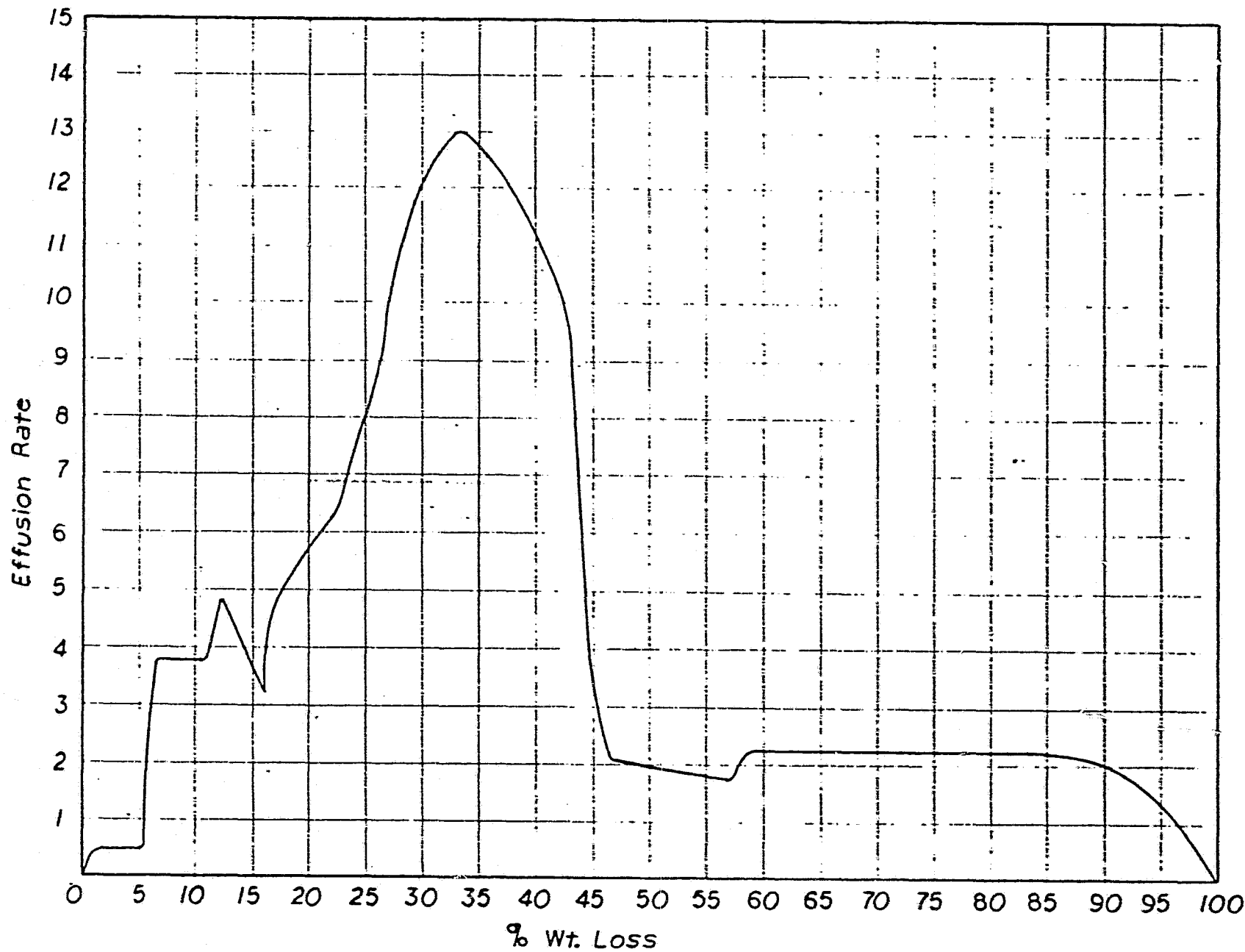
Figure 13. Isothermal Rate-of-Effusion vs. Fraction Vaporized. K_2S at $780^\circ C$ in Alumina Cell.
Rates are Relative.

before 50% of the sample was depleted in order to avoid the maximum of Fig. 12. This strategy was adopted on the assumption that the effusion behavior of the isothermal experiments was due to an effect other than that of equilibrium vaporization for which measurements were sought.

2.3.4 K$_2$S Effusion from Graphite Knudsen Cells

The results of Table VIII appear in the order they were acquired. After "point" number 12, subsequent effusion rates (points 13-21) were lower by almost a factor of 2 (Fig. 14). Such an abrupt fall-off in the rate-of-effusion of K$_2$S was also observed in effusion studies at UT (Ref. 3). In that work we attributed the higher rates to the incongruent reaction (10) for which the effusant is predominantly K(g). The lower rates were assigned to the onset of the congruent vaporization of K$_2$S$_4$(c).

$$K_2S_4(c) = 2K(g) + 2S_2(g) \tag{13}$$

Results in Table VIII do not provide information about whether K$_2$S$_4$ is formed as a congruently vaporizing phase, but they do indicate that a change in the vaporization reaction occurs.

2.3.5 Comparison of K$_2$S and K$_2$SO$_3$ Effusion Results

The disproportionation reaction (7) suggests that vapor species and effusion rates for K$_2$SO$_3$ and K$_2$S should be the same in the range $\sim$ 700-1000°C. This comparison is complicated by possible contributions to the vaporization of K$_2$SO$_3$ from reactions (5) and (8), and by possible solution effects between K$_2$S and K$_2$SO$_4$ (Ref. 10). Comparison of calculated vapor pressures (Figs. 8 and 14), and of mass spectra (Figs. 6

Table VIII

Rates-of-Effusion and Vapor Pressures for
K_2S Vaporization from a Graphite Knudsen Cell

#	10^{10} x Rate, kg/s	°K	10^6 x P, atm
1	1.74	1063	12.0
2	1.81	1063	12.5
3	1.79	1063	12.4
4	2.81	1078	19.6
5	4.23	1093	29.7
6	5.72	1108	40.4
7	8.11	1123	57.7
8	4.17	1093	29.3
9	8.07	1123	57.4
10	10.5	1138	75.2
11	15.6	1163	113.
12	20.5	1178	149.
13	0.333	998	2.23
14	1.79	1078	12.5
15	2.48	1093	17.4
16	4.36	1123	31.0
17	8.33	1158	60.2
18	11.5	1173	83.6
19	6.47	1148	46.5
20	10.6	1173	77.1
21	1.62	1073	11.3

(1) Pyrolytic graphite-coated graphite Knudsen cell, orifice area $1.70 \times 10^{-7} M^2$
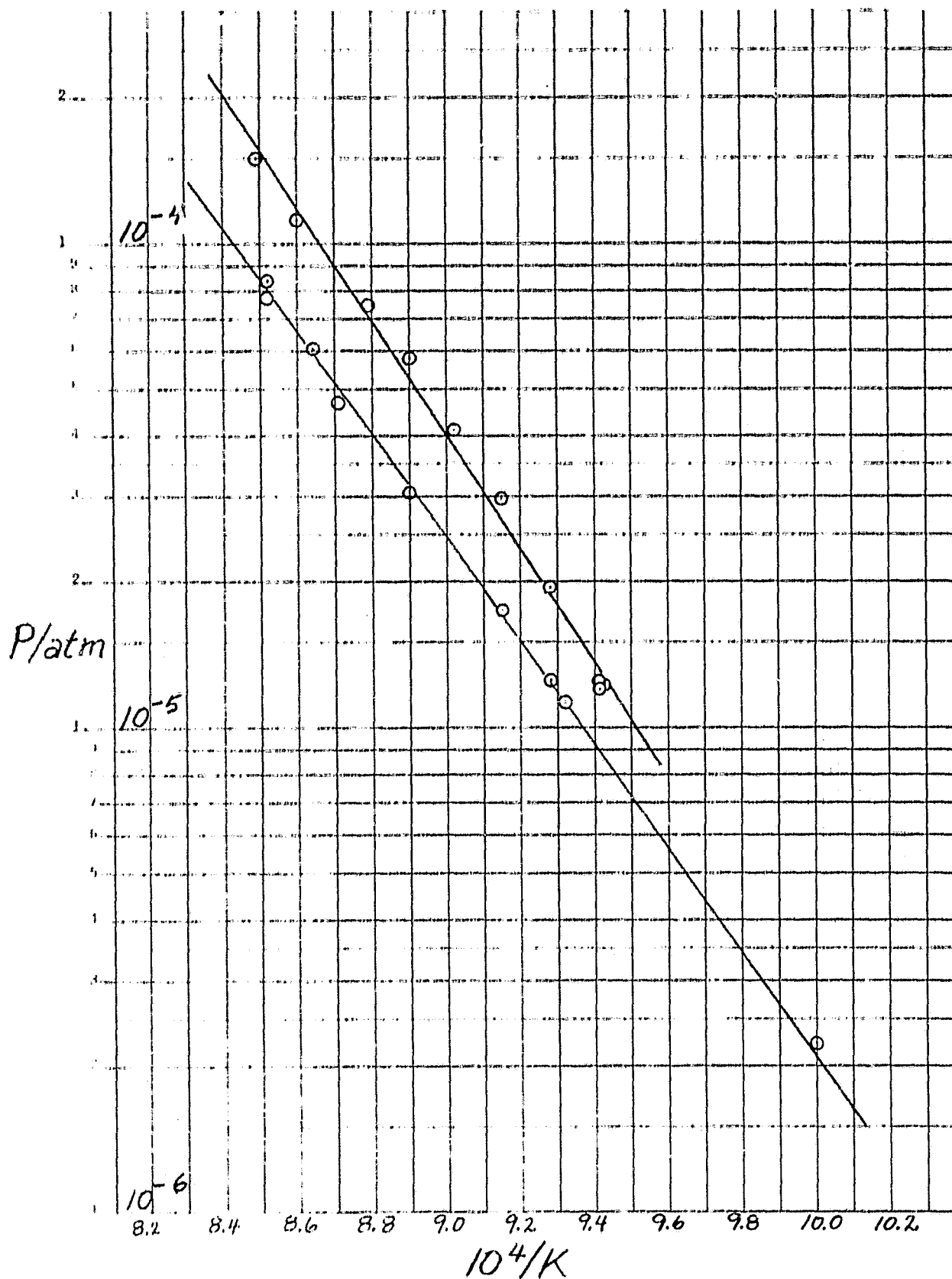(2) Points #1-12 apply to reaction (10).
(3) Points #13-21 apply to reaction (11).

Figure 14. Log P(atm) vs $10^4/T$ for Vaporization of K_2S in a Graphite Knudsen Cell.

and 10), however, shows a striking similarity, as predicted by comparing reactions (7) and (10).

2.4 THERMODYNAMIC CALCULATIONS

The accumulated results from these studies indicate that the early stages of vaporization of both K_2SO_3 and K_2S involve $K(g)$ as the predominant gaseous species, in accordance with reaction (10). The value of x for calculations was taken as x = 4 in our previous report (Ref. 3). This value was based on effusion data by Edwards at UT which indicated the formation of a congruently vaporizing phase of composition K_2S_4. While the present results cannot shed light on the K_2S_4 congruency, the value x = 4 nevertheless appears a reasonable value because of the closeness in ΔH_f^0 values reported for K_2S_x (Ref. 11):

$$K_2S_2 \quad \Delta H_f^0, \ 298 = -103.0 \pm 0.7 \ kcal/mole$$

$$K_2S_3 \quad \Delta H_f^0, \ 298 = -111.8 \pm 1.2 \ kcal/mole$$

$$K_2S_4 \quad \Delta H_f^0, \ 298 = -111.3 \pm 0.5 \ kcal/mole$$

$$K_2S_5 \quad \Delta H_f^0, \ 298 = -112.2 \pm 0.4 \ kcal/mole$$

$$K_2S_6 \quad \Delta H_f^0, \ 298 = -111.9 \pm 0.7 \ kcal/mole$$

Within experimental error, the above results indicate that ΔH_f^0 (298) is the same for all K_2S_x when x > 2. The initial vaporization reaction, applicable to both K_2S and K_2SO_3, may be written in terms of one mole of gaseous product as

$$2/3 \ K_2S(s) \ = 1/6 \ K_2S_4(1) + K(g) \tag{14}$$
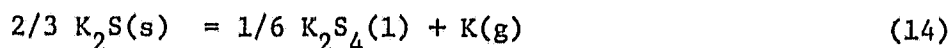
for which the equilibrium constant K_p (assuming unit activity for

condensed phases) is simply

$$K_p = P \tag{15}$$

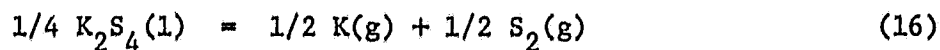The first set of pressures in Table VIII, calculated by the method of equation (1), apply to reaction (14), and yield a least squares fit of

$$\log P(atm)(reaction\ 14) = -11920/T + 6.336$$

The second set of pressures in Table VIII corresponds to reaction (11) which becomes for one mole of gaseous product

$$1/4\ K_2S_4(1) = 1/2\ K(g) + 1/2\ S_2(g) \tag{16}$$

with

$$K_p = P_K^{1/2}P_{S_2}^{1/2} = 0.5P \tag{17}$$

The pressure data for reaction (16) yields a least squares fit of

$$\log P(atm)(reaction\ 16) = -10400/T + 4.756$$

Standard deviations for the least squares equations provide uncertainties of about ±2%.

The value for ΔH_f° (298) of $K_2S(s)$ can be calculated by combining the results of third law calculations applied to reactions (14) and (16). The third law equation

$$\Delta H^\circ_{298} = -RT\ln K_p - T\Delta\phi \tag{18}$$

requires free energy functions ϕ for all species in (16) and (17). All ϕ's are available from the JANAF Tables (Ref. 12) except those for $K_2S_4(1)$, which we estimated previously (Ref. 3) by the following relationships:

$$\phi[K_2S_4(s)] = \phi[K_2S(s)] + 3(\phi[Na_2O_2(s)] - \phi[Na_2O(s)]) \tag{19}$$

$$\phi[K_2S_4(1)] = \phi[K_2S_4(s) + 2(\phi[Na_2S(1)] - \phi[Na_2S(s)]) \tag{20}$$

46

Table IX

Free-Energy Functions

$$\phi^o = -[G^o - H^o(298K)]/T \ (cal/mol \ K)$$

T(K)	K(g)	S_2(g)	K_2S(s)	K_2S_4(ℓ)	$\Delta\phi^o$ React (10)	React (11)
900	40.46	58.11	35.73	59.11	26.48	34.51
1000	40.82	58.73	37.21	62.21	26.39	34.22
1100	41.16	59.31	38.75	65.18	26.19	33.94
1200	41.48	59.86	40.32	68.01	25.93	33.67
1300	41.78	60.38	41.86	70.40	25.61	33.48

Table X

Heats of Formation of K_2S and K_2SO_3

Compound	Source	Reference	Method	ΔH_f^o, 298 (kcal mol^{-1})
$K_2S(s)$	Sabatier, 1881	(13)	Sol'n Calorimetry	−103.4
	Rengade & Costeanu, 1914	(14)	Sol'n Calorimetry	− 87.3
	Letoffe, et al., 1974	(11)	Sol'n Calorimetry	− 92.1
	JANAF, 1978	(12)	Compilation	− 90.0±3
	Ortman, et al., 1979	(9)	Mass Spectrometry	− 90.3±2.4
	Johnson & Steele, 1981	(15)	F_2 Calorimetry	− 97.1±0.6
$K_2SO_3(s)$	Berthelot, 1884, Martin & Metz; NBS Circular 500	(16)	Experimental	−266.9
	Erdös, 1962	(17)	Estimation	−267.2
	Rasch, 1970; Barin & Knacke (5)	(18)	Estimation	−272.0

By this method we obtained:

$$\Delta H^{\circ}_{298}, \text{ reaction (14)} = 53.4 \pm 0.09 \text{ kcal mol}^{-1}$$

$$\Delta H^{\circ}_{298}, \text{ reaction (16)} = 64.9 \pm 0.05 \text{ kcal mol}^{-1}$$

Free energy functions ϕ used in these calculations appear in Table IX. These results, when combined with JANAF values for ΔH°_f (298) of K(g) and of S_2(g) (21.31 and 30.71 kcal mol^{-1}, respectively), give ΔH°_f (298) for K_2S(s): -87.1 ± 3.0 kcal mol^{-1} as reported previously (Ref. 3) using vapor pressures obtained at UT, and -82.0 ± 3 kcal mol^{-1} using pressures from Table VIII. Results from other sources (Table X) support the first value above. The source of our different results (ASU vs UT) lies in the measured vapor pressures (and thus the RT&nK terms) for K_2S, for which the ASU results were consistently higher than those from UT. The reason for the difference in measured pressures is not understood.

3. SUGGESTIONS FOR FUTURE WORK

The high temperature chemistry of K_2SO_3 and K_2S is complex, as reflected by the paucity of thermodynamic data which provided the impetus for this work. Measurements at high temperatures are affected by interaction with container materials, usually in ways not understood, as in the boron nitride results for K_2SO_3, and the alumina results for K_2S. It is not clear that a suitable container material has yet been found, and future studies will have to deal with this problem. The most desirable extension of the present work, however, would be studies of K_2SO_4 in graphite containers. Such studies would provide a critical test for the reaction sequence that our results support for K_2SO_3 in graphite, and the necessary experiments should be straightforward. On the basis of our findings, for example, one would predict that K_2SO_4(s) would as the result of reaction (9) "vaporize" from a graphite Knudsen cell at say $800°C$, which is too low a temperature (m.p. K_2SO_4, $1069°C$) for the true vaporization of K_2SO_4. This reaction should be of much interest in MHD seed-cycle considerations.

More complex studies suggested by this work would involve elucidation of the "peaks" from the isothermal total exhaustion experiments of section 2.3.3. Those results are probably kinetically rather than thermodynamically controlled, as evidenced by numerous increases in effusion rates (and thus of vapor pressures) at constant temperatures. The effect of surface to volume ratios of the samples, which were quite small in the isothermal experiments, would probably also require investigation.

4. PUBLICATIONS AND PRESENTATIONS

4.1 PROGRESS REPORTS

1. Project Status Report, July 13, 1979

2. First Semi-Annual Report, January 11, 1980

3. Second Semi-Annual Report, June 1980

4. Third Semi-Annual Report, February 3, 1981

4.2 PUBLICATION

1. J. E. Bennett, V. S. Chincholkar, J. G. Edwards, L. E. Grimes, R. Haque, F. J. Kohl, F. Sibieude, and C. A. Stearns, "Vaporization Thermodynamics of K_2S and K_2SO_3," in Proceedings of the Symposium on High Temperature Materials Chemistry, ed. by D. D. Cubicciotti and D. L. Hildenbrand, Proceedings Volume 82-1, The Electrochemical Society, Pennington, NJ, 1982, pp. 337-352.

4.3 THESIS

1. W. M. Simpson, "Vaporization of K_2SO_3 and Implementation of CEC71," Arkansas State University, M.S. Thesis, 1982.

4.4 PRESENTATIONS

1. J. E. Bennett, "Experimental Confirmation of the Incongruent Vaporization of K_2S at High Temperatures," 66th Annual Meeting of the Arkansas Academy of Science, Arkadelphia, AR, April 1982.

2. J. E. Bennett, V. S. Chincholkar, J. G. Edwards, L. E. Grimes, R. Haque, F. J. Kohl, F. Sibieude, and C. A. Stearns, "Vaporization Thermodynamics of K_2S and K_2SO_3," presented at the 160th Meeting of the Electrochemical Society, Denver, CO, October 1981, Paper No. 453.

3. J. E. Bennett, "Knudsen Mode Thermogravimetric Analysis," Ninth Midwest High Temperature Chemistry Conference, Los Alamos, NM, June 1981.

4. J. E. Bennett, "Knudsen Mode High Temperature Thermogravimetric Analysis," 65th Annual Meeting of the Arkansas Academy of Science, Little Rock, AR, April 1981.

5. W. M. Simpson and J. E. Bennett, "Tube Furnace Studies of the Vaporization Reaction of K_2SO_3," 65th Annual Meeting of the Arkansas Academy of Science, Little Rock, AR, April 1981.

6. J. E. Bennett and W. M. Simpson, "An Experimental System for the Determination of Vaporization Kinetics and Thermodynamics at Temperatures to $3300^{\circ}K$," 64th Annual Meeting of the Arkansas Academy of Science, Jonesboro, AR, March 1980.

7. W. M. Simpson and J. E. Bennett, "Implementation of the NASA Chemical Equilibrium Program at Arkansas State University," 64th Annual Meeting of the Arkansas Academy of Science, Jonesboro, AR, March 1980.

5. ADDENDUM

Reaction of potassium sulfate with graphite. Discovery of the disproportionation reaction of K_2SO_3 in graphite containers

$$4K_2SO_3 = K_2S + 3K_2SO_4 \qquad (1A)$$
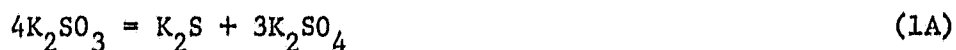
raised questions about possible subsequent reactions of K_2SO_4 with graphite. No reference to K_2SO_4-graphite reactions were found in the literature, but the significance of such reactions was perceived to be of sufficient importance to this work to justify experimental studies. Results from these studies came too late for the main body of this report. Instead the essential findings are summarized in this addendum.

Tube furnace experiments were conducted in which K_2SO_4-graphite mixtures in a graphite Knudsen cell were subjected to high temperatures under high vacuum in an arrangement such that vapors effusing from inside the cell were caused to deposit on the inner walls of a Vycor tube. The Vycor tube possessed a temperature gradient that ranged from room temperature to the temperature of the furnace hot zone, thus causing selective deposition of vapors. Reaction occurred with visibly discernible deposits at about 780°C. Deposits (in order of increasing distance from the hot zone) were found to be: 1) mixture of potassium sulfides; 2) elemental sulfur; 3) elemental potassium. This kind of experiment was repeated three times at temperatures to 850°C, and the results in each case were as described above. Similar experiments were then carried out in a vacuum furnace equipped with a quadrupole mass spectrometer probe. The permanent gases CO and CO_2 were detected with the quadrupole as products of the reaction between K_2SO_4 and graphite above about 750°C. These gases were not detectable in the tube furnace

experiments because they did not condense under the conditions of those experiments. Species assigned from positive ion spectrometry as originating from the Knudsen cell were (in order of decreasing intensity): CO_2, CO, K, S_2, O. Below about 800°C the CO intensity was greater than that of CO_2, but above this temperature the intensities reversed. Species looked for but not detected were: SO_2, SO_3, O_2, S_4, S_6, S_8, S_{10}. Minute non-background signals were obtained for K_2S_x, with x = 1,2,3,4,5,6, but uncertainties were too great for meaningful assignments.

These results indicate that the reaction between K_2SO_4 and graphite proceeds according to

$$K_2SO_4(s) + 4C(gr) = 4CO + K_2S \qquad (2A)$$

and $\qquad K_2SO_4(s) + 2C(gr) = 2CO_2 + K_2S \qquad (3A)$
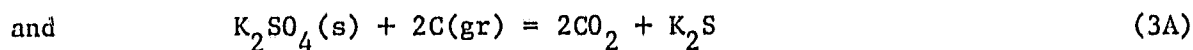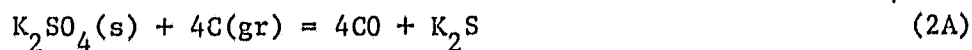
with subsequent incongruent vaporization of K_2S (as described in this report). X-ray powder diffraction of cell residues gave only K_2SO_4 patterns, thus indicating against the idea of K_2SO_3 as an intermediate of (2A) and (3A). It is possible that only (3A) occurs and that CO(g) results solely from the decomposition of CO_2(g), but this has not been established. We do attribute the detected species O(g), however, as resulting from either the reduction or the decomposition of CO_2, and not from K_2SO_4.

6. REFERENCES

1. J. E. Bennett, F. J. Kohl, C. A. Stearns, G. C. Fryburg, and J. A. Burkhart, DOE/NASA/2674-79/1, NASA TM-79114, 1979.

2. J. B. Heywood and G. J. Womack, eds., Open Cycle MHD Power Generation. Pergamon Press, Inc., pp 662,665, 1969.

3. J. E. Bennett, V. S. Chincholkar, J. G. Edwards, L. E. Grimes, R. Haque, F. J. Kohl, F. Sibieude, and C. A. Stearns, "Proceedings of the Symposium on High Temperature Materials Chemistry," The Electrochemical Society, Proceeding Vol 82-1, p 337-52, 1982.

4. J. L. Margrave , ed., The Characterization of High Temperature Vapors. John Wiley and Sons, Inc., 1967.

5. S. Gordon and B. J. McBride, Computer Program for Calculation of Complex Chemical Equilibrium Compositions, NASA SP-273, 1971.

6. R. Hultgren et al, Selected Values of the Thermodynamic Properties of the Elements, American Society for Metals, Metals Park, OH, 252.

7. L. E. Grimes, M. S. Thesis, with J. G. Edwards, Univ. of Toledo, 1981.

8. A. S. Dworkin and M. A. Bredig, J. Phys. Chem. 71, 764 (1967).

9. B. Ortman, Mass Spectrometric Studies of the K_2S System, Division of Chemical Engineering, Argonne National Laboratory, DOE W-31-109-ENG-38 (1978).

10. C. W. So and D. Barham, J. Therm. Anal. 20, 275 (1981).

11. J. M. Letoffe et al, J. Chim. Phys. Physicochim. Biol. 71, 427 (1974).

12. M. W. Chase et al, JANAF Thermochemical Tables, Dow Chemical Company, Midland, MI, and Supplements to 1979.

13. P. Sabatier, Annls. Chim. Phys., Ser. 5 22, 5 (1881).

14. E. Rengade and N. Costeanu, Compt. Rend. 158, 946 (1914); Bull. Soc. Chim. Fr. 15, 717 (1914).

15. G. K. Johnson and W. V. Steele, J. Chem. Thermodynamics 13, 985 (1981).

16. References in F. D. Rossini et al, Selected Values of Chemical Thermodynamic Properties, Circular 500, National Bureau of Standards, Washington, DC, 1952.

17. E. Erdös, Collection Czechoslov. Chem. Commun. 27, 1428 (1962).

18. R. Rasch, Sprechsall 103, 117 (1970).